In situ click chemistry-based rapid discovery of novel HIV-1 NNRTIs by exploiting the hydrophobic channel and tolerant regions of NNIBP

Dongwei Kang, Da Feng, Lanlan Jing, Yanying Sun, Fenju Wei, Xiangyi Jiang, Gaochan Wu, Erik De Clercq, Christophe Pannecouque, Peng Zhan, Xinyong Liu

PII: S0223-5234(20)30204-X

DOI: https://doi.org/10.1016/j.ejmech.2020.112237

Reference: EJMECH 112237

To appear in: *European Journal of Medicinal Chemistry*

Received Date: 16 February 2020

Revised Date: 11 March 2020

Accepted Date: 11 March 2020

Please cite this article as: D. Kang, D. Feng, L. Jing, Y. Sun, F. Wei, X. Jiang, G. Wu, E. De Clercq, C. Pannecouque, P. Zhan, X. Liu, *In situ* click chemistry-based rapid discovery of novel HIV-1 NNRTIs by exploiting the hydrophobic channel and tolerant regions of NNIBP, *European Journal of Medicinal Chemistry* (2020), doi: https://doi.org/10.1016/j.ejmech.2020.112237.

Graphical abstract

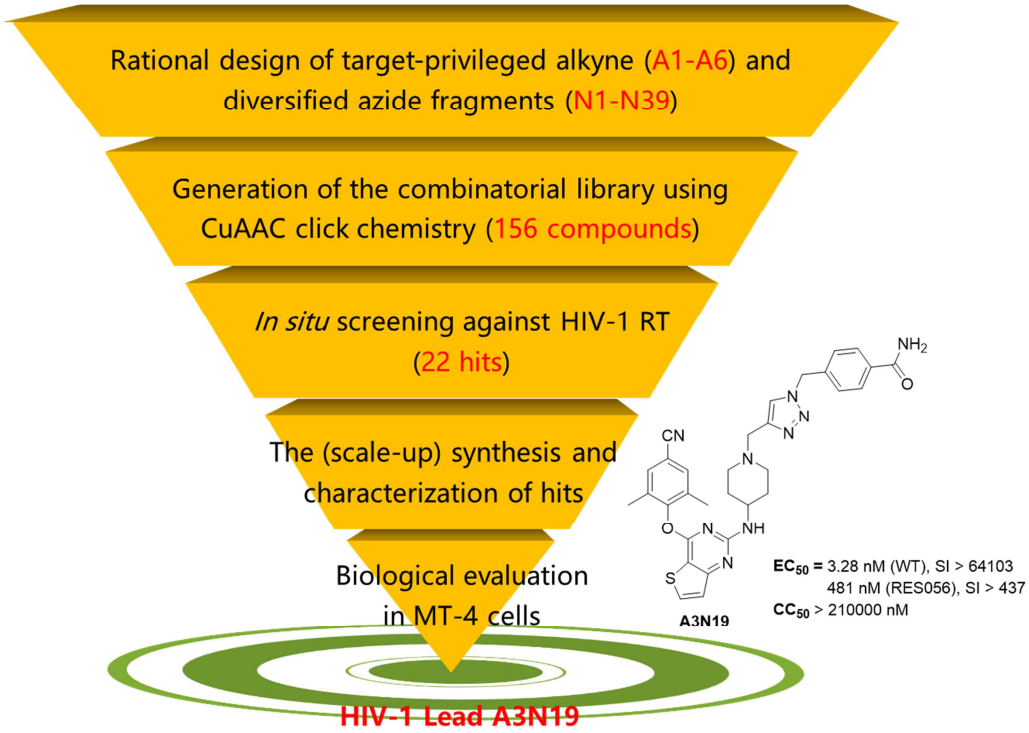

Discovery of potent HIV-1 NNRTIs from CuAAC click-chemistry-based combinatorial libraries

In Situ Click Chemistry-Based Rapid Discovery of Novel HIV-1 NNRTIs By Exploiting the Hydrophobic Channel and Tolerant Regions of NNIBP

Dongwei Kang,[†, &,ω] Da Feng, [†] Lanlan Jing,[†] Yanying Sun,[†] Fenju Wei,[†] Xiangyi Jiang,[†] Gaochan Wu,[†] Erik De Clercq, [§] Christophe Pannecouque,[§] Peng Zhan[†,&,*] and Xinyong Liu,[†, &,*]

[†] *Department of Medicinal Chemistry, Key Laboratory of Chemical Biology (Ministry of Education), School of Pharmaceutical Sciences, Shandong University, 44 West Culture Road, 250012 Jinan, Shandong, PR China*

[§] *Rega Institute for Medical Research, Laboratory of Virology and Chemotherapy, K.U. Leuven, Herestraat 49 Postbus 1043 (09.A097), B-3000 Leuven, Belgium.*

[&]*China-Belgium Collaborative Research Center for Innovative Antiviral Drugs of Shandong Province, 44 West Culture Road, 250012 Jinan, Shandong, PR China*

[ω] *Suzhou Research Institute, Shandong University, Room522, Building H of NUSP, NO.388 Ruoshui Road, SIP, Suzhou, 215123 Jiangsu, P.R. China*

ABSTRACT:

HIV-1 RT has been considered as one of the most important targets for the development of anti-HIV drugs for their well-solved three-dimensional structure and well-known mechanism of action. In this study, with HIV-1 RT as target, we used miniaturized parallel click chemistry synthesis *via* CuAAC reaction followed by *in situ* biological screening to discover novel potent HIV-1 NNRTIs. A 156 triazole-containing inhibitor library was assembled in microtiter plates and in millimolar scale. The enzyme inhibition screening results showed that 22 compounds exhibited improved inhibitory activity. Anti-HIV-1 activity results demonstrated that **A3N19** effected the most potent activity against HIV-1 IIIB (EC_{50} = 3.28 nM) and

mutant strain RES056 (EC_{50} = 481 nM). The molecular simulation analysis suggested that the hydrogen bonding interactions of **A3N19** with the main chain of Lys101 and Lys104 was responsible for its potency. Overall, the results indicated the *in situ* click chemistry-based strategy was rational and might be amenable for the future discovery of more potent HIV-1 NNRTIs.

Keywords: HIV-1, DAPY, NNRTIs, *In situ* screening, CuAAC, Click Chemistry

1. INTRODUCTION

According to the Joint United Nations Program on HIV/AIDS (UNAIDS) report 2018, more than 37.9 million people are today living with human immunodeficiency virus (HIV), including 1.7 million people newly infected with HIV in 2018.[1] HIV infection is still pandemic around the world. Among all the targets for treatment HIV-1 disease, reverse transcriptase (RT) has been considered as one of the most successful. Especially, non-nucleoside reverse transcriptase inhibitors (NNRTIs) have gained a definitive place due to their unique antiviral potency, high specificity, and low toxicity in highly active antiretroviral therapy (HAART) used to treat HIV.[2, 3] According to UNAIDS, 62% of people living with HIV were receiving antiretroviral treatment in 2018.[1] So far, more than 50 structurally diverse classes of inhibitors have been identified as HIV-1 NNRTIs. They could non-competitive interact with the allosteric site (known as the non-nucleoside inhibitory binding pocket, NNIBP) of HIV-1 RT, and then induce conformational changes of the catalytic domain to inhibit their DNA polymerase activity.[4, 5] Among them, six NNRTIs were approved for AIDS therapy. Nevirapine (NVP), delavirdine (DLV) and efavirenz (EFV) are

first-generation NNRTIs, etravirine (ETR), rilpivirine (RPV), and doravirine (DOR) are second-generation NNRTIs.[6, 7] However, the first-generation NNRTIs encountered a sharp loss of activity with mutants such as Y181C, K103N and RES056 (Y181C+K103N), and the second-generation NNRTIs show loss of activity against single-point mutations such as K101E and E138K.[8] In addition, hypersensitivity reactions or other adverse effects have been reported with second-generation NNRTIs.[9] Therefore, the development of novel NNRTIs with more active potency, increased resistance profiles and less toxicity is still highly desired.

High-throughput screening (HTS) of compounds libraries has always been a widely used approach for drug discovery, based on the construction of a high-quality compounds library.[10] Various new synthetic methodologies and concepts have been proposed for the assembly of compound collections.[11] Among them, click chemistry, especially copper(I)-catalyzed azide–alkyne (3 + 2) dipolar cycloaddition (CuAAC), is generally regarded as a powerful fragment-based assembly reaction for rapid synthesis of small molecules libraries with its unique advantages, such as mild reaction conditions, almost complete chemoselectivity with broad functional group tolerance, excellent yield and excellent biorthogonality, which means the CuAAC could rapid generate a triazole-containing compounds library for activity screening without purification.[12-14] In recent years, the rapid assembly and *in situ* screening of focused combinatorial fragment libraries using CuAAC click chemistry has become more robust, and an efficient strategy for bioactive molecules generation. [15-17] Although various strategies have been made to seek novel anti-HIV-1

inhibitors,[18, 19] there has been no previous report on the discovery of novel NNRTIs based on *in situ* click chemistry. In this work, we report for the first time the rapid identification of highly potent HIV-1 NNRTIs with this technique.

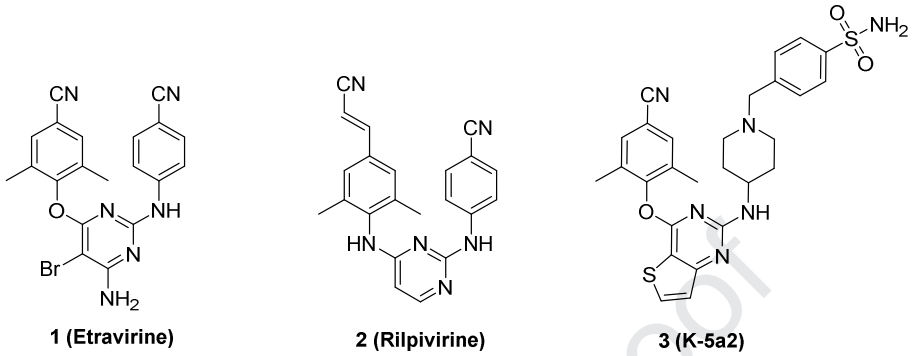

Figure 1. Chemical structures of U.S. FDA-approved second-generation NNRTI drugs (**1** and **2**) and our previously reported potent HIV-1 NNRTI **K-5a2**.

Our previous efforts have led to the development of a novel potent thiophene[3,2-*d*]pyrimidine NNRTIs **K-5a2**.[20] The co-crystal structure of HIV-1 wild-type (WT) RT in complex with **K-5a2** revealed that **K-5a2** adopted a horseshoe conformation in the NNIBP, and displayed remarkable structural complementarity to the NNIBP with substantial extensions into the three channels, namely hydrophobic channel, tolerant region I and tolerant region II, which is similar to that observed with ETR.[21] Specifically, the left wing of **K-5a2** arches into the tunnel lined by Tyr181, Tyr188, Phe227, and Trp229, forming π-π interactions with these residues. The piperidine-linked aryl structure of the right wing projects into the groove surrounded by Lys103, Val106, Pro225, Pro236, and Tyr318, establishing van der Waals contacts with their lipophilic side chains. The terminal sulfonamide group extends to the solvent-exposed surface and forms hydrogen-bonding with the backbone of Lys104 and Val106. The thiophene[3,2-*d*]pyrimidine heterocyclic

structure of **K-5a2** located at the tolerant region II formed by Glu138 and Lys101, developing novel nonpolar interactions with the alkyl chain of Glu138. Furthermore, the nitrogen atoms in the central thiophene pyrimidine and the amine group linking the central thiophene pyrimidine and the piperidine ring develops double hydrogen-bonding network with the carbonyl oxygen of Lys101, which plays an important role in maintaining its high anti-HIV activity.

In this article, with **K-5a2** and ETR as lead compounds, six alkyne building block (**A1-A6**) were designed to further exploit the hydrophobic channel and tolerant regions of NNIBP and discover novel NNRTIs with greater potency.[22-25] Moreover, according to the chemical space of the three-dimensional structure of NNIBP, azide substituents **N1-36** and **N34-39** with different aryl substituents varying in size, polar group substitution, and electronic nature were designed to match the tolerant regions and hydrophobic channel, respectively. Then CuAAC click chemistry in 96-wall plates provided triazoles-containing derivatives, which were tested for HIV- RT inhibitory activity directly without purification. Further *in vitro* anti-HIV activity evaluation and molecular docking led to the identification of compound **A3N19** as a promising lead compound.

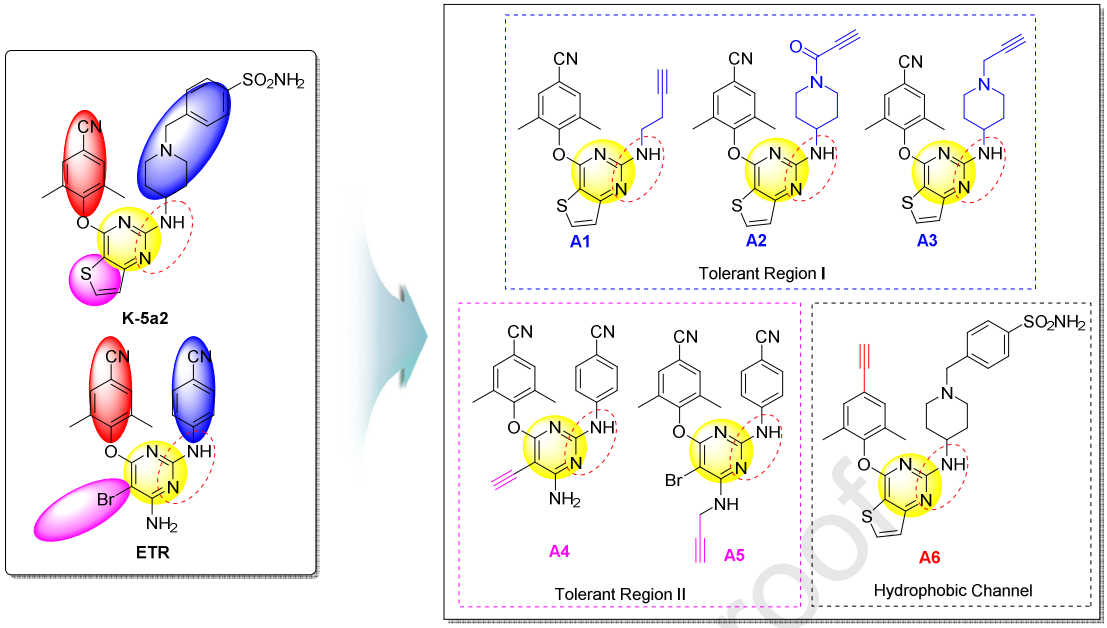

Figure 2. Design of alkynes based on the co-crystal structure of HIV-1 RT/K-5a2 and RT/ETR

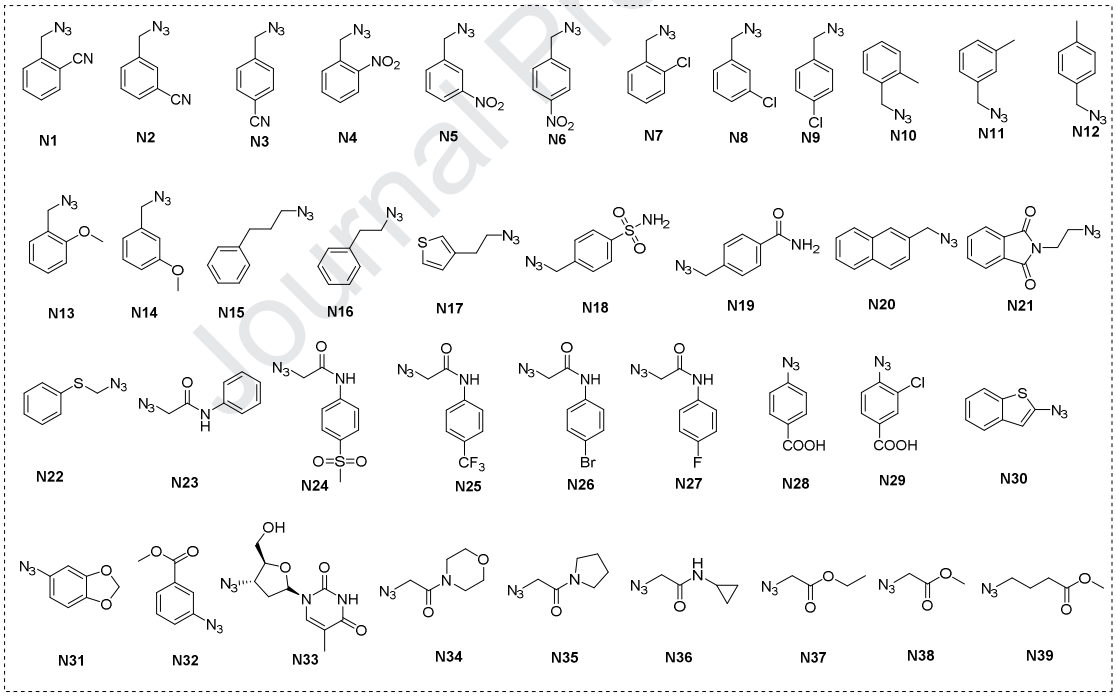

Figure 3. Structures of the designed diverse azide substituents

2. RESULTS AND DISCUSSION

2.1 Building and characterizing the libraries by click chemistry

The general synthetic steps adopted to obtain the alkynes **A1–6** are outlined in

Scheme 1-5. As depicted in **Scheme 1**, with our previously reported compound **4** as starting material,[26] the alkyne building block **A1** was obtained underwent a S_NAr reaction with but-3-yn-1-amine. Treatment of compounds **5** with propargyl bromide in DMF at room temperature afforded alkynes **A2**, while **A3** was obtained by treatment **5** with propiolic acid using HATU as condensation agent.

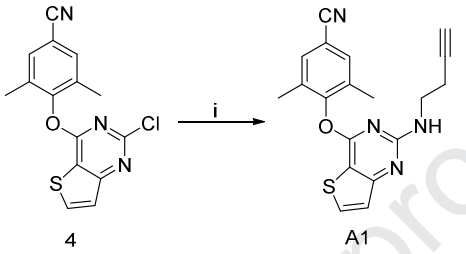

Scheme 1. Reagents and conditions (i) K_2CO_3, DMF, but-3-yn-1-amine, 80°C, 59%.

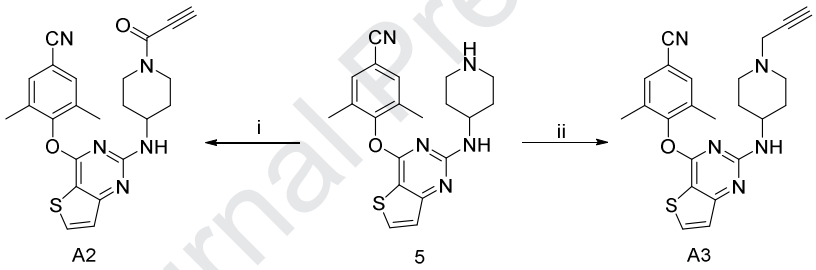

Scheme 2. Reagents and conditions (i) HATU, propiolic acid, DCM, r.t., 62%; (ii) K_2CO_3, DMF, propargyl bromide, r.t., 71%.

As shown in **Scheme 3**, the starting material 2,4,6-trichloropyrimidine **6** was treated with 4-hydroxy-3,5-dimethylbenzonitrile to give the compound **7**, which following reaction with 4-aminobenzonitrile provided the intermediate **8**. Subsequent ammonolysis reaction using $NH_3.H_2O$ in NMP *via* a microwave reaction yielded compound **9**, which was converted to the key intermediate **11** using PbO_2 and I_2 in HOAc. Then, the target alkyne building block **A4** was prepared from **11** *via* the Sonogashira cross-coupling and trimethylsilyl-removal reaction.

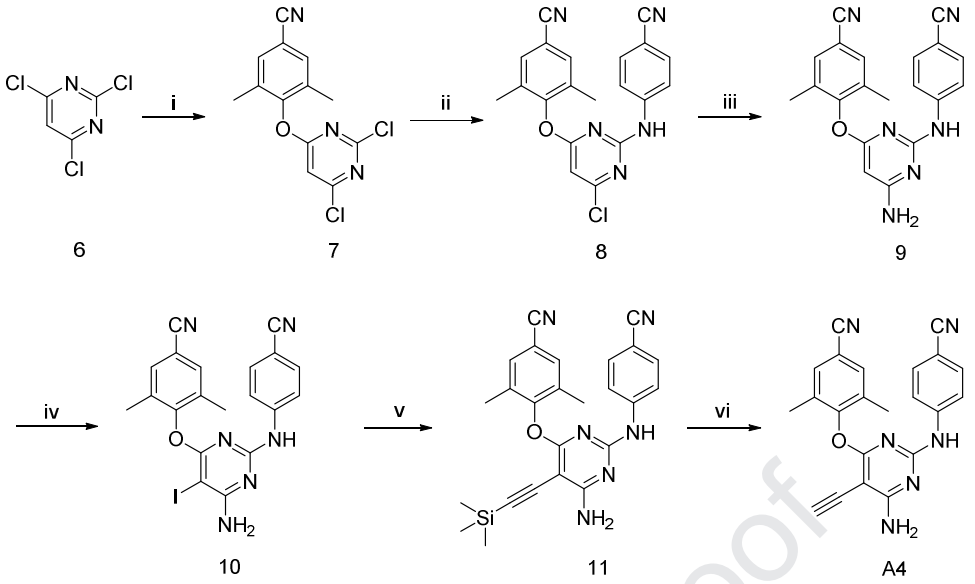

Scheme 3. Reagents and conditions (i) 3,5-dimethyl-4-hydroxybenzonitrile, 1,4-dioxane, 70°C, 2 h, 92%; (ii) 4-aminobenzonitrile, NMP, t-BuOK, 0-5°C, 60%; (iii) $NH_3.H_2O$, NMP, 130°C, 15 min, mw, 85%; (iv) PbO_2, I_2, HOAc, r.t., 64%; (v) ethynyltrimethylsilane, $PdCl_2(PPh_3)_2$, CuI, Et_3N, THF, r.t.; (vi) K_2CO_3, MeOH, r.t., 72%.

The approved drug ETR reacted with 3-bromopropyne in the presence of K_2CO_3 obtained **A5** (**Scheme 4**). Synthesis of alkyne building block **A6** is shown in **Scheme 5**. Firstly, nucleophilic substitution of 2,4-dichlorothiophene[3,2-*d*]pyrimidine (**12**) with 4-iodo-2,6-dimethylphenol and 4-Boc-aminopiperidine in the presence of K_2CO_3 and DMF afforded the key intermediate **14**. Deprotection with trifluoroacetic acid in dichloromethane gave compound **15**, which was reacted with 4-(bromomethyl)benzenesulfonamide to obtain intermediate **16**. Then, the target alkyne building block **A6** was prepared from **16** *via* the Sonogashira cross-coupling and trimethylsilyl-removal reaction. The synthesis of azide is detailed in our previously published paper.[17]

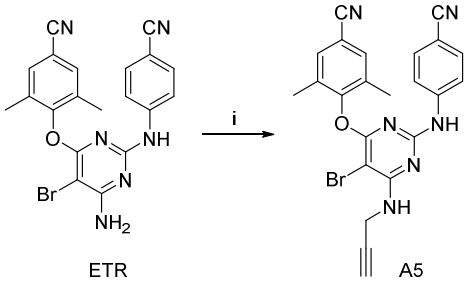

Scheme 4. Reagents and conditions (i): K_2CO_3, DMF, propargyl bromide, r.t., 63%.

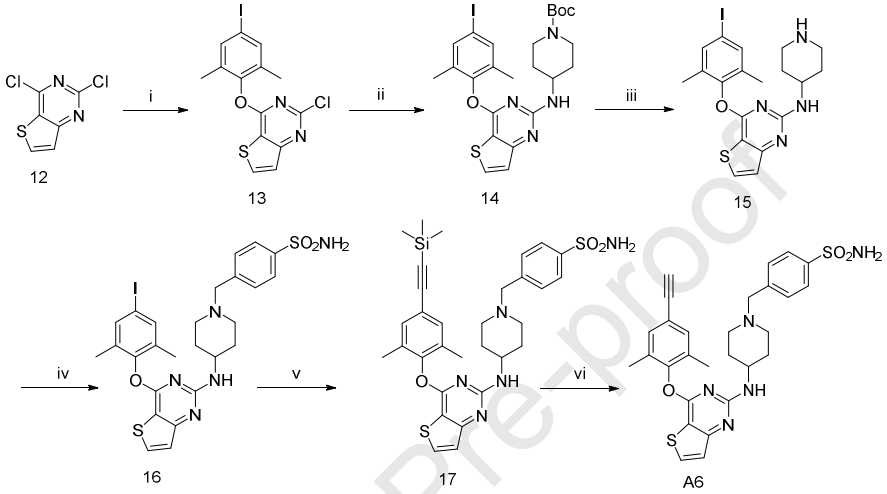

Scheme 5. Reagents and conditions (i): 4-iodo-2,6-dimethylphenol, K_2CO_3, DMF, r.t., 89%; (ii) *tert*-butyl 4-aminopiperidine-1-carboxylate, K_2CO_3, DMF, 120°C; (iii) TFA, DCM, r.t., 68%; (iv) K_2CO_3, DMF, r.t., 75%; (v) ethynyltrimethylsilane, $PdCl_2(PPh_3)_2$, CuI, Et_3N, THF, 50°C; (vi) K_2CO_3, MeOH, r.t., 54%.

2.2. Generation of the combinatorial library

Using the CuAAC reaction, a 156 triazole-containing inhibitor library was assembled in microtiter plates and at millimolar scale. Each of the **A1-A4** alkynes was mixed with each of the **N1-N36** azides and **A5**, **A6** alkynes were mixed with each of the **N34-N39** azides in DMSO solution, followed by the addition of catalytic amounts of tris[(1-benzyl-1*H*-1,2,3-triazol-4-yl)methyl]amine (TBTA), $CuSO_4 \cdot 5H_2O$ and sodium ascorbate (VcNa). The detailed reaction conditions and dosage of the reactants are shown in **Table 1**. The completion of the reaction was detected by TLC (about 24

hours). The compounds are shown in the supporting information **Table S1**.

Table 1. Detailed reaction conditions.

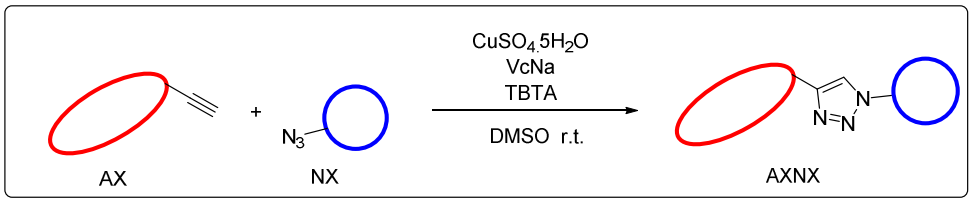

Reagents	Concentration	Volume	Final Concentration
Alkyne-unit (Ax)	25 mM DMSO	20 μL	5 mM
Azide-unit (Nx)	35 mM DMSO	20 μL	7 mM
TBTA	10 mM DMSO	10 μL	20 mol%
$CuSO_4.5H_2O$	4 mM MilliQ	25 μL	20 mol%
VcNa	20 mM MilliQ	25 μL	100 mol%
Total Volume		100 μL/well	

2.3. *In situ* screening against HIV-1 RT

With the aim to rapidly discover novel potent HIV-1 NNRTIs, the generated triazole-containing library was screened for their HIV-1 RT inhibitory activity at 0.267 μM (final concentration) without further purification. The lead compounds ETR and K-5a2 were selected as reference drugs, a mixture solution of TBTA, $CuSO_4 \cdot 5H_2O$ and VcNa was used as blank control. As shown in **Figures 4-7**, a total of 22 hits emerged from the screens. For the A1 alkyne building block, the inhibition percentages of **A1N4** (89.1%), **A1N7** (75.6%), **A1N11** (91.8%), **A1N18** (72.4%), **A1N19** (71.1%) and **A1N34** (86.7%) were higher than **ETR** (62.3%) and **K-5a2** (56.2%) against HIV-1 RT. In the case of the A2 alkyne building block, only three compounds showed higher enzyme activity, including **A2N10** (75.8%), **A2N23** (80.2%), and **A2N34** (71.8%). For the **A3** alkyne building block, **A3N1** (50.3%),

A3N4 (51.9%), **A3N10**(44.8%), **A3N12**(46.1%), **A3N18**(42.0%), **A3N19** (66.6%), **A3N24** (60.1%), **A3N33** (57.1%), **A3N34** (69.7%) and **A3N35** (73.0 %) exhibited greater enzyme inhibitory activity than ETR (32.7%) and K-5a2 (44.0%). **A6NX**, which was designed for exploiting the hydrophobic channel of the NNIBP, **A6N9** (70.8%), **A6N17** (72.5%) and **A6N35** (74.0 %) showed improved inhibitory activity compared to ETR (64.0%) and K-5a2 (58.7%). However, compounds **A4NX** and **A5NX** showed decreased enzyme activity (**Supporting Information Table S2**).

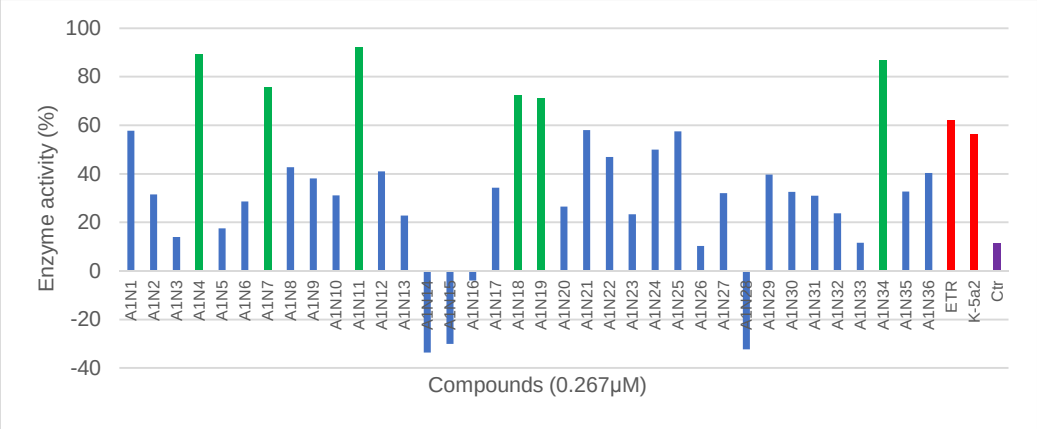

Figure 4. HIV-1 RT inhibitory activity in the presence of 0.267 μM **A1NX**

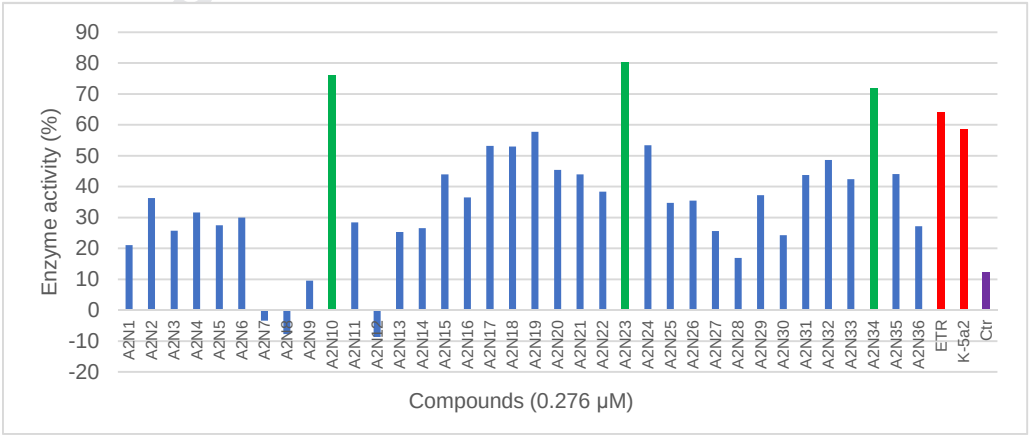

Figure 5. HIV-1 RT inhibitory activity in the presence of 0.267 μM **A2NX**

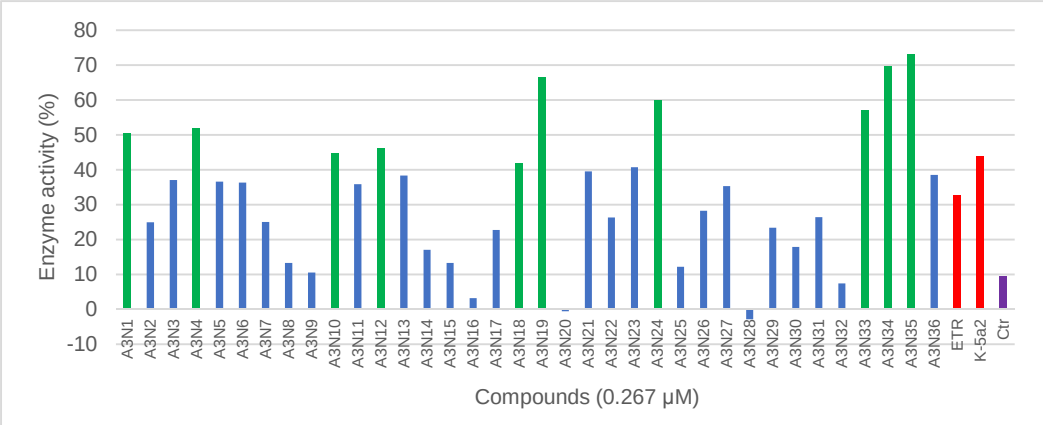

Figure 6. HIV-1 RT inhibitory activity in the presence of 0.267 μM **A3NX**

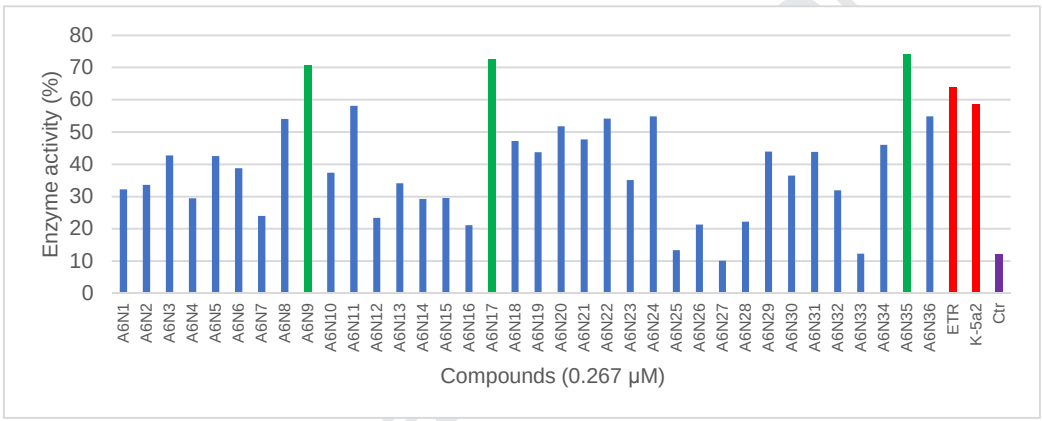

Figure 7. HIV-1 RT inhibitory activity in the presence of 0.267 μM **A6NX**

2.4. Biological evaluation

Then the selected 22 hits were individually re-synthesized at a milligram scale with the aim to perform further biological studies at the cellular level. In addition, we also synthesized compound **A3N3** with the aim to verify the correlation between enzyme activity and cell activity. Their *in vitro* antiviral potency was evaluated in MT-4 cell cultures infected with WT HIV-1 strain (IIIB) as well as cells infected with double-mutant strains K103N+Y181C (RES056). NVP, EFV, and ETR were selected as control drugs, and **K-5a2** was selected as the reference compound. The values of EC_{50} (anti-HIV potency), CC_{50} (cytotoxicity) as well as SI (selectivity index,

CC_{50}/EC_{50} ratio) of the synthesized compounds are summarized.

The anti-HIV-1 activity results demonstrated that **A3** was the most preferred alkyne building block. As depicted in **Table 2**, most compounds of the **A3NX** series exhibited potent activity against HIV-1 IIIB with low nanomolar EC_{50} values ranging from 3.28 to 10.4 nM, being far more potent than the reference drug NVP (EC_{50} = 163 nM). **A3N19** (EC_{50} = 3.28 nM) and **A3N34** (EC_{50} = 4.38 nM) turned out to be the most potent HIV-1 inhibitors, being comparable to the drug EFV (EC_{50} = 4.7 nM), ETR (EC_{50} = 5.1 nM) and the lead K-5a2 (EC_{50} = 1.63 nM). Moreover, **A3N19** and **A3N34** exhibited no cytotoxicity (CC_{50}) up to the maximum tested concentration of 210 and 212 μM, which contribute to their higher SI values (SI > 64103 and 48544, respectively). It is noteworthy that compound **A3N3** displayed much decreased potency again HIV-1 IIIB with an EC_{50} value of 209 nM. Compounds **A6N9**, **A6N17** and **A6N35** exhibited modest antiviral activity with EC_{50} values of 31.3, 21.1 and 25.8 nM, respectively.

In the case of mutant HIV-1 strain RES056, **A3N18** and **A3N19** exhibited modest potency of 670 nM and 481 nM, being comparable to that of EFV (EC_{50} = 264 nM) but inferior to that of ETR (EC_{50} = 45.4 nM). The other compounds are almost inactive to RES056. In addition, the antiviral results also demonstrated that compounds **A1NX** and **A2NX** showed sharply reduced activity against HIV-1 IIIB and RES056 (**See the Supporting information, Table S3**).

Table 2. Activity and cytotoxicity against WT HIV-1 (IIIB) and mutant strain RES056

Compds	EC_{50} (nM)[a]		CC_{50} (μM)[b]	SI[c]		Inhibition Ration
	IIIB	RES056		IIIB	RES056	
A3N1	6.64±1.15	2911±431	16.2±7.01	2444	6	0.503
A3N3	209±65.5	18053±1512	110±3.92	525	6	0.370
A3N4	6.12±0.87	1173±147	7.66±2.79	1252	7	0.519
A3N10	10.4±1.3	>4760	4.76±0.19	454	<1	0.448
A3N12	7.26±1.61	>4720	4.72±0.22	650	<1	0.461
A3N18	5.35±0.35	670±0.33	20.7±0.66	3881	31	0.420
A3N19	3.28±0.83	481±16.2	>210	>64103	>437	0.666
A3N24	6.66±1.34	1994±240	19.8±1.09	2974	10	0.601
A3N33	82.9±23.9	10555±385	149±6.90	1800	14	0.571
A3N34	4.38±0.65	4464±1258	>212	>48544	>48	0.697
A3N35	5.02±2.08	7032±1174	117±3.68	23325	17	0.730
A6N9	31.3±11.3	>3395	3.39±0.31	108	<1	0.708
A6N17	21.1±7.03	6186±670	11.7±5.35	552	1.88	0.725
A6N35	25.8±7.32	6046±840	17.6±4.23	682	3	0.740
K-5a2	1.4±0.4	30.6±12	>227	>159101	>53533	0.442
NVP	163±41.2	>9513	>9.51	>58	NA [d]	-
ETR	5.1±0.8	45.4±15.5	>4.59	>889	>101	0.327
EFV	4.7±1.7	264±27.3	>6.38	>1333	>24	-

[a] EC_{50}: concentration of compound required to achieve 50% protection of MT-4 cell cultures against HIV-1-induced cytopathic effect, as determined by the MTT method.

[b] CC_{50}: concentration required to reduce the viability of mock-infected cell cultures by 50%, as determined by the MTT method.

[c] SI: selectivity index, the ratio of CC_{50}/EC_{50}.

[d] NA: not available.

2.5 Molecular modeling analysis

With the aim to obtain insight into the allosteric binding of the novel designed derivatives to the NNIBP, the molecular docking studies for representative compounds **A3N19** and **A3N34** was performed by using the software SurflexeDock SYBYL-X

2.0. PyMOL was used to visualize the docking results. Co-crystal structure of HIV-1 WT RT/K-5a2 (PDB code: 6c0n) and RES056 RT/K-5a2 (PDB code: 6c0r) were used as the input structures for docking calculations.[21] The docking protocol is described in the computational section.

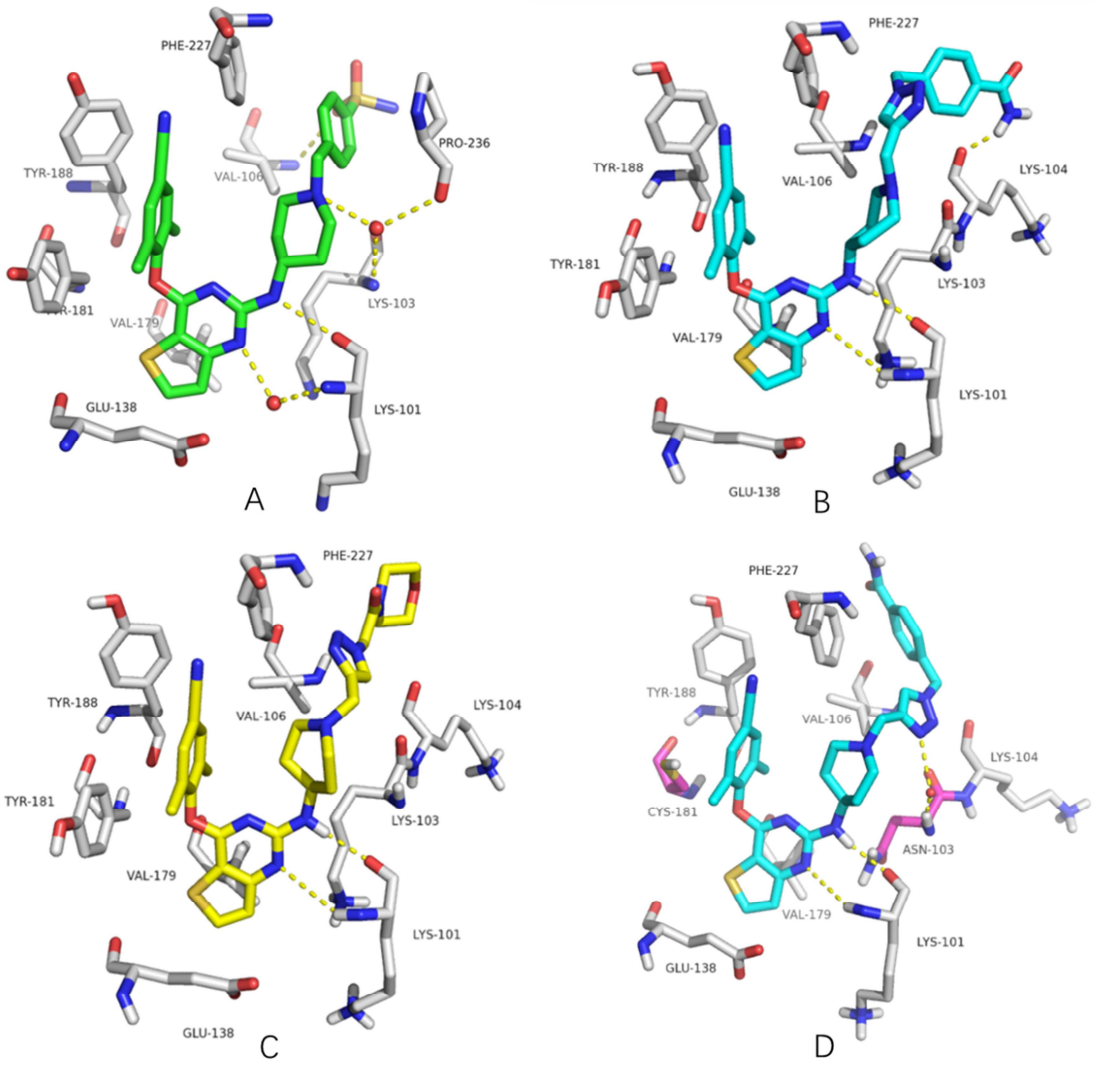

Figure 8. The binding mode of lead K-5a2 (**A**), the predicted binding modes of **A3N19** (**B**) and **A3N34** (**C**) with the HIV-1 WT RT (PDB code: 6c0n), and the predicted binding mode of **A3N19** with the HIV-1 RES056 RT (**D**, PDB code: 6c0r). The hydrogen bonds are indicated with yellow dashed lines.

The docking simulations of **A3N19** and **A3N34** with HIV-1 WT RT (PDB code:

6c0n) demonstrated that their binding modes were similar with the lead K-5a2 (**Figure 8**). Firstly, the left 4-cyano-2,6-dimethylphenyl group of **A3N19** and **A3N34** occupies the hydrophobic sub-pocket composed by aromatic amino acid residues Tyr181, Tyr188, and Phe227, exhibiting aryl-aryl interaction with these residues. Secondly, the central thiophene[3,2-*d*]pyrimidine heterocycle effectively occupies the NNIBP tolerant regions II, establishes nonpolar interactions with the alkyl chain of Glu138 and favorable hydrophobic contacts with Val179. Thirdly, the *NH* linker connecting the central pyrimidine ring and the right wing and pyrimidine nitrogen develops a dual hydrogen bond with the main chain backbone of Lys101. Notably, the sulfonamide group of the lead K-5a2 forms double-hydrogen bonding with the carbonyl oxygen of Lys104 and the backbone nitrogen of Val106, while the amide group of **A3N19** yields hydrogen-bonding interactions with the main chain of Lys104 and the morpholine ring of **A3N34** does not establish any hydrogen bond interactions, which may responsible for their decreased activity for WT HIV-1 strain. In regard to RT carrying the more disruptive RES056 double-mutation (PDB code: 6c0r), the Y181C mutation abolishes the most favorable π-π interaction between the Tyr181 side chain and the dimethyl phenyl ring of **A3N19**. In addition, the terminal substituent of **A3N19** is twisted and lost the hydrogen bonding with Lys104. Although the triazole group developed novel hydrogen bonding through a water molecular with the mutant ASN103, it was not enough to compensate for the loss of the foremost π-π interaction and the hydrogen bonding with the minichain of Lys104. All these may be account for the decreased anti-HIV-1 activities against HIV-1 RES056.

Furthermore, by comparing the binding mode of **A3N19** and **A3N34** with WT and RES056 RT, we conclude that the newly introduced hydrogen bond receptor triazole group plays pivotal role of keeping their terminal substituent in a reasonable conformation in the NNIBP. In turn, the terminal substituent of the compounds also influence the conformation of triazole, which means that it could be regarded as a dominant site for structural modification to establish stronger hydrogen bonding interactions between the triazole and NNIBP. The docking simulations contribute to understand the binding mode of the newly designed compounds with NNIBP, which helps further structure-based design of novel potent NNRTIs.

3. CONCLUSION

In conclusion, we reported the identification of highly potent HIV-1 NNRTIs from miniaturization CuAAC click-chemistry-based combinatorial libraries. In this exploratory project, 22 hits emerged from the enzyme-inhibitory screening, and were then synthesized and evaluated for their anti-HIV-1 activity *in vitro*. All these efforts led to the successful discovery of a potent HIV-1 NNRTI, **A3N19**, which exhibited active potency against WT HIV-1 IIIB (EC_{50} = 3.28 nM) and mutant strain RES056 (EC_{50} = 481 nM). Moreover, **A3N19** exhibited lower cytotoxicity (CC_{50} > 210 μM) and higher SI values (SI > 64103, HIV-1 IIIB). The project indicates this *in situ* click chemistry-based strategy was rational and might be amenable for the future discovery of more potent HIV-1 NNRTIs. In addition, the molecular simulation analysis suggested that the strong activity profile of **A3N19** against WT and mutant HIV-1 strains can be attributed to its hydrogen bonding interactions with the main chain of

Lys101 and Lys104.

4. EXPERIMENTAL SECTION

4.1. Chemistry

4-((2-(but-3-yn-1-ylamino)thieno[3,2-*d*]pyrimidin-4-yl)oxy)-3,5-dimethylbenzonitrile (A1)

The starting material **4** (1.0 mmol, 0.32 g) was treated with but-3-yn-1-amine (1.2 mmol, 0.08 g) in the presence of anhydrous K_2CO_3 (2.0 mmol, 0.28 g) in 10 mL DMF. The mixture was stirred at 80°C for 8 h (monitored by TLC). The solution cooled to room temperature and 40 mL water was added. Then the mixture was extracted with ethyl acetate (3 × 15 mL) and the organic phase was dried over anhydrous Na_2SO_4. The solvent concentrated in vacuo and the crude product was purified by flash column chromatography to yield the target compound **A1** with a yield of 59%, mp: 203-205□. ^{1}H NMR (400 MHz, DMSO-d_6): δ 8.11 (d, J = 5.3 Hz, 1H, C_6-thienopyrimidine-H), 7.72 (s, 2H, C_3,C_5-Ph-H), 7.29 (d, J = 5.4 Hz, 1H, C_7-thienopyrimidine-H), 6.04 (s, 1H, NH), 4.34-4.32 (m, 2H, N-CH_2), 2.87(s, 1H), 2.32-2.28 (m, 2H), 2.10 (s, 6H). ^{13}C NMR (100 MHz, DMSO-d_6): δ 168.0, 162.1, 160.8, 153.6, 133.6, 132.2, 129.3, 126.7, 125.2, 119.1, 108.6, 82.2, 71.8, 50.3, 30.1, 21.5, 16.2. ESI-MS: m/z 349.2 $[M + 1]^+$. $C_{19}H_{16}N_4OS$ (348.10).

3,5-dimethyl-4-((2-((1-propioloylpiperidin-4-yl)amino)thieno[3,2-*d*]pyrimidin-4-yl)oxy)benzonitrile (A2)

Our previously reported compound **5** (0.5 mmol, 0.19 g) was selected as starting material,[26] which was treated with HATU (0.6 mmol, 0.22 g), propiolic acid (0.6

mmol, 0.04 g) in 5 mL of dry DCM and stirred at room temperature. After the reaction was completed, the solvent was removed under reduced pressure. Then the residue was washed with 30 mL saturated aqueous sodium chloride and DCM (3 × 10 mL), the organic layer was separated, dried over Na_2SO_4 and filtered. The concentrated product was purified by flash column chromatography to give the target compound **A2** with a yield of 62%, mp: 254-256□. ^{1}H NMR (400 MHz, DMSO-d_6, ppm): δ 8.11 (d, J = 5.4 Hz, 1H, C_6-thienopyrimidine-H), 7.76 (d, J = 8.3 Hz, 2H, C_3,C_5-Ph-H), 7.72 (s, 2H, C_3,C_5-Ph'-H), 7.41 (d, J = 8.4 Hz, 2H, C_2,C_6-Ph-H), 7.31 (s, 2H, SO_2NH_2), 7.25 (d, J = 5.4 Hz, 1H, C_7-thienopyrimidine-H), 6.04 (s, 1H, NH), 3.75-3.74 (m, 1H), 2.72-2.70 (m, 2H), 2.12 (s, 6H), 1.95-1.45 (m, 6H). ^{13}C NMR (100 MHz, DMSO-d_6): δ 165.0, 163.1, 160.9, 153.7, 153.1, 143.3, 136.7, 133.6, 133.0, 129.3, 126.8, 123.8, 123.1, 119.0, 109.6, 61.9, 52.8, 31.8, 16.2. ESI-MS: m/z 432.3 $[M + 1]^+$. $C_{23}H_{21}N_5O_2S$ (431.14).

3,5-dimethyl-4-((2-((1-(prop-2-yn-1-yl)piperidin-4-yl)amino)thieno[3,2-*d*] pyrimidin-4-yl)oxy)benzonitrile (A3)

A mixture of **5** (0.5 mmol, 0.19 g) anhydrous K_2CO_3 (1.0 mmol, 0.14 g) and 3-bromoprop-1-yne (0.6 mmol, 0.07 g) in 5 mL DMF was stirred at room temperature for 8 h (monitored by TLC), and then saturated sodium chloride solution (20 mL) was added. The mixture was extracted with ethyl acetate (3 × 15 mL) and the organic phase was dried over anhydrous Na_2SO_4. The solvent concentrated in vacuo and the crude product was purified by flash column chromatography. The product was recrystallized from ethyl acetate/petroleum ether to afford the target compound **A3**

with a yield of 71%, mp: 272-274□. ^{1}H NMR (400 MHz, DMSO-d_6) δ 8.20 (d, J = 5.3 Hz, 1H, C_6-thienopyrimidine-H), 7.72 (s, 2H, C_3,C_5-Ph-H), 7.27 (s, 1H, C_7-thienopyrimidine-H), 6.88 (s, 1H, NH), 3.69 (s, 1H), 3.22 (s, 2H, N-CH_2), 3.13 (s, 1H, CH≡), 2.74 (s, 2H), 2.12 (s, 6H), 1.90-1.30 (m, 6H). ^{13}C NMR (100 MHz, DMSO-d_6) δ 162.4, 160.5, 153.4, 133.2, 132.9, 123.7, 119.0, 109.0, 75.9, 51.3, 46.6, 31.5, 16.2. ESI-MS: m/z 418.5 $[M + 1]^+$. $C_{23}H_{23}N_5OS$ (417.16).

4-((2,6-dichloropyrimidin-4-yl)oxy)-3,5-dimethylbenzonitrile (7)

2,4,6-trichloropyrimidine (**6**, 11 mmol, 2.0 g), DIEPA (13 mmol, 1.7 g) and 4-hydroxy-3,5-dimethylbenzonitrile (11 mmol, 1.6 g) were dissolved in 10 mL 1,4-dioxane and the mixed solution were heated at 70°C for 2 h. After the reaction mixture was brought to room temperature, 50 mL cold water was poured into the mixture and stirred for another 30 min, filtrated. The wet cake was dried at 55-60°C under vacuum to give the intermediate 7 as white solid with a yield of 92%, mp: 207-209℃. ^{1}H NMR (400 MHz, DMSO-d_6, ppm) δ: 7.76 (s, 2H, C_3,C_5-Ph-H), 7.64 (s, 1H, pyrimidine-H), 2.12 (s, 6H). ESI-MS: m/z 294.2 $[M + 1]^+$. $C_{13}H_9Cl_2N_3O$ (293.01).

4-((6-chloro-2-((4-cyanophenyl)amino)pyrimidin-4-yl)oxy)-3,5-dimethylbenzonitrile (8)

The obtained intermediate **7** (6.8 mmol, 2.0 g) and 4-aminobenzonitrile (6.8 mmol, 0.8 g) were dissolved in NMP (10 mL) at 0-5°C, then the solution was added potassium *tert*-butoxide (13.6 mmol, 1.53 g) over a period of 30 min and stirred for another 2 h at 0-5°C. Then the mixture was added to 50 mL cold water slowly and

filtered to get white precipitate, which was suspended in cold water (30 mL) and acidified to pH 6-7 with 3M HCl. The formed solid was filtered, dried at 55-60°C under vacuum to give the crude product, which was subsequently washed with 20 mL ethyl acetate. Then the wet cake was finally dried at 50°C under vacuum to give the intermediate **8** as white solid with a yield of 60%, mp: 277-279℃. ^{1}H NMR (400 MHz, DMSO-d_6, ppm) δ: 10.56 (s, 1H, NH), 7.79 (s, 2H, C_3,C_5-Ph'-H), 7.55-7.45 (m, 4H), 6.93 (s, 1H, pyrimidine-H), 2.13 (s, 6H). ESI-MS: m/z: 376.5 $[M + 1]^+$, 393.3 $[M + NH_4]^+$. $C_{20}H_{14}ClN_5O$ (375.09).

4-((6-amino-2-((4-cyanophenyl)amino)pyrimidin-4-yl)oxy)-3,5-dimethylbenzonitrile (9)

Intermediate **8** (0.53 mmol, 0.20 g) and 25% aq ammonia (15 mL) were dissolved in 20 mL NMP and the mixture solution was put into a microwave reactor in 130°C for 15 min. In the reaction process, the pressure of this reaction system can up to 135 psi. After the reaction mixture was brought to 5-10°C, 15 mL cold water was added and stirred for another 30 min. The yielded solid was filtered, washed with 15 mL water and dried at 45-50°C to give the intermediate **9** as white solid with a yield of 85%, mp: 283-286℃. ^{1}H NMR (400 MHz, DMSO-d_6, ppm) δ: 9.57 (s, 1H, NH), 7.73 (s, 2H, C_3,C_5-Ph'-H), 7.65 (d, J = 8.0 Hz, 2H, C_3,C_5-Ph-H), 7.46 (d, J = 8.0 Hz, 2H, C_2,C_6-Ph-H), 6.80 (s, 2H, NH_2), 5.47 (s, 1H, pyrimidine-H), 2.12 (s, 6H). ESI-MS: m/z 357.4 $[M + 1]^+$, 379.5 $[M + Na]^+$. $C_{20}H_{16}N_6O$ (356.14).

4-((6-amino-2-((4-cyanophenyl)amino)-5-iodopyrimidin-4-yl)oxy)-3,5-dimethylbenzonitrile (10)

Intermediate **9** (0.84 mmol, 0.3 g) was dissolved in 5 mL glacial acetic acid, then PbO_2 (0.30 mmol, 0.07 g) and I_2 (0.30 mmol, 0.08 g) were added and the mixed solution was stirred at room temperature for 4 h. Then the reaction mixture was diluted with H_2O and stirred for another 30 min, the obtained precipitate was filtered, washed with H_2O. Then the crude product was purified by flash column chromatography to obtain **10** with a yield of 64%, mp: 302-304□. ^{1}H NMR (400 MHz, DMSO-d_6) δ 9.58 (s, 1H, NH), 7.74 (s, 2H, C_3,C_5-Ph'-H), 7.55 (d, *J* = 8.5 Hz, 2H, C_3,C_5-Ph-H), 7.43 (d, *J* = 8.5 Hz, 2H, C_2,C_6-Ph-H), 6.98 (s, 2H, NH_2), 2.11 (s, 6H). ^{13}C NMR (100 MHz, DMSO-d_6) δ 166.8, 165.5, 158.5, 154.9, 145.4, 133.1, 132.9, 132.8, 120.0, 119.1, 118.6, 108.6, 102.4, 46.8, 16.2. ESI-MS: m/z 483.4 $[M + 1]^+$. $C_{20}H_{15}IN_6O$ (482.04).

4-((6-amino-2-((4-cyanophenyl)amino)-5-ethynylpyrimidin-4-yl)oxy)-3,5-di methylbenzonitrile (A4)

Compound **10** (1.0 mmol, 0.48 g), $PdCl_2(PPh_3)_2$ (0.05 mmol, 0.04 g), CuI (0.2 mmol, 0.04 g) and triethylamine (4.0 mmol, 0.5 mL) were added to 10 mL THF. Then trimethylsilylacetylene (2.2 mmol, 0.2 g) was added to the mixed solution under N_2 and stirred at room temperature for 24 h. Then the mixture was filtered through a celite pad. The filtrate was concentrated and purified by flash column chromatography to afford the key intermediate **11**. Then **11** was added 5 mL MeOH and potassium carbonate (7 mmol, 1.1g), and the mixture was stirred at room temperature for 1h. To the reaction mixture was added 10 mL saturated sodium bicarbonate solution, filtrated and the solid was washed with water. The crude product was recrystallized in MeOH

to get the target product **A4** as white solid with a yield of 72%, mp: 295-297□. ^{1}H NMR (400 MHz, DMSO-d_6) δ 9.58 (s, 1H, NH), 7.74 (s, 2H, C_3,C_5-Ph'-H), 7.55 (d, J = 8.5 Hz, 2H, C_3,C_5-Ph-H), 7.43 (d, J = 8.5 Hz, 2H, C_2,C_6-Ph-H), 6.98 (s, 2H, NH_2), 3.24 (s, 1H, CH≡), 2.11 (s, 6H). ^{13}C NMR (100 MHz, DMSO-d_6) δ 166.8, 165.5, 158.5, 154.9, 145.6, 133.1, 132.9, 132.7, 120.0, 119.1, 118.6, 108.7, 102.4, 81.6, 73.4, 46.8, 16.2. ESI-MS: m/z 381.5 $[M + 1]^+$. $C_{20}H_{16}N_6O$ (380.14).

4-((5-bromo-2-((4-cyanophenyl)amino)-6-(prop-2-yn-1-ylamino)pyrimidin-4-yl)oxy)-3,5-dimethylbenzonitrile (A5)

The approved drug ETR (0.5 mmol, 0.22 g) was selected as starting material and dissolved in 10 mL anhydrous DMF in the presence of anhydrous K_2CO_3 (1.0 mmol, 0.14 g) and 3-bromoprop-1-yne (0.6 mmol, 0.07 g). The mixture was stirred at room temperature for 5 h (monitored by TLC), and then the solvent was removed under reduced pressure. The residue was taken up in water (20 mL) and extracted with ethyl acetate (3 × 10 mL). The organic phase was dried over anhydrous Na_2SO_4, filtered, and purified by flash column chromatography. The product was recrystallized from ethyl acetate/petroleum ether to afford the target compound **A5** with a yield of 63%, mp: 264-267□. ^{1}H NMR (400 MHz, DMSO-d_6) δ 9.58 (s, 1H, NH), 7.74 (s, 2H, C_3,C_5-Ph'-H), 7.55 (d, J = 8.5 Hz, 2H, C_3,C_5-Ph-H), 7.43 (d, J = 8.5 Hz, 2H, C_2,C_6-Ph-H), 7.36 (s, 1H), 3.93-3.66 (m, 2H, N-CH_2), 2.94 (s, 1H, CH≡), 2.10 (s, 6H). ^{13}C NMR (100 MHz, DMSO-d_6) δ 166.8, 165.5, 158.5, 154.9, 145.5, 133.1, 132.9, 132.8, 120.0, 119.2, 118.6, 108.8, 102.4, 82.1, 72.4, 30.6, 16.2. ESI-MS: m/z 473.4 $[M + 1]^+$. $C_{23}H_{17}BrN_6O$ (472.06).

2-chloro-4-(4-iodo-2,6-dimethylphenoxy)thieno[3,2-*d*]pyrimidine (13)

A mixture of 2,4-dichlorothiopheno[3,2-*d*]pyrimidine (**12**, 1.0 mmol, 0.21 g), 4-iodo-2,6-dimethylphenol (1.0 mmol, 0.25 g), and anhydrous K_2CO_3 (1.2 mmol, 0.17 g) in 5 mL DMF was stirred at 25°C for 2 h (monitored by TLC). The mixture was poured into ice water and then the obtained precipitate was collected by filtration, recrystallized in DMF-H_2O to provide the product **13** as white solid in 89 % yield, mp: 243-245°C. ESI-MS: m/z 417.1 $[M + 1]^+$. $C_{14}H_{10}ClIN_2OS$ (415.92).

4-(4-iodo-2,6-dimethylphenoxy)-*N*-(piperidin-4-yl)thieno[3,2-*d*]pyrimidin-2-amin e (15)

A solution of **13** (1.0mmol, 0.42 g), *N*-Boc-4-aminopiperidine (1.2 mmol, 0.24 g), and anhydrous K_2CO_3 (2.0 mmol, 0.28 g) in DMF (5 mL) was heated at 120°C for 12 h (monitored by TLC). Then the solution was cooled to room temperature, and 30 mL ice water was added. The resulting precipitate was collected by filtration, and dried to give crude **14,** which was used directly in the next step without further purification. To a solution of **14** (1.2 mmol, 0.70 g) in DCM (4 mL) was added trifluoroacetic acid (10 mmol, 0.74 mL), and the solution was stirred at room temperature for 4 h (monitored by TLC). The reaction solution was alkalized to pH 9 with saturated sodium bicarbonate solution and the aqueous phase was extracted with DCM (3×10 mL). The combined organic phase was dried over anhydrous Na_2SO_4, filtered and purified by flash column chromatography to give **15** as a yellow solid in 68% yield, mp: 125-127°C. ESI-MS: m/z 481.3 $[M + 1]^+$. $C_{19}H_{21}IN_4OS$ (480.05).

4-((4-((4-(4-iodo-2,6-dimethylphenoxy)thieno[3,2-*d*]pyrimidin-2-yl)amino)

piperidin-1-yl)methyl)benzenesulfonamide (16)

Compound **15** (1.0 mmol, 0.48 g), 4-(bromomethyl)benzenesulfonamide (1.1 mmol, 0.27 g) and anhydrous K_2CO_3 (1.2 mmol, 0.16 g) were dissolved in 10 mL anhydrous DMF. The reaction mixture was stirred at room temperature for 5 h and then 50 mL water was added, extracted with ethyl acetate (3×10 mL), and the organic phase was dried over anhydrous Na_2SO_4, purified by flash column chromatography to afford compound **16** as a white solid in 75% yield, mp: 279-181°C. ESI-MS: m/z 650.5 $[M + 1]^+$. $C_{26}H_{28}IN_5O_3S_2$ (649.07).

4-((4-((4-(4-ethynyl-2,6-dimethylphenoxy)thieno[3,2-*d*]pyrimidin-2-yl)amino) piperidin-1-yl)methyl)benzenesulfonamide (A6)

Compound **16** (1.0 mmol, 0.45 g), $PdCl_2(PPh_3)_2$ (0.05 mmol, 0.04 g), CuI (0.2 mmol, 0.04 g) and Et_3N (4.0 mmol, 0.5 mL) were added to 10 mL THF. Then trimethylsilylacetylene (2.2 mmol, 0.2 g) was added to the solution under N_2 and stirred at 50°C for 8 h. Then the mixture was filtered, concentrated and purified by flash column chromatography to afford the key intermediate **17**. Then **17** was treated with K_2CO_3 (7.0 mmol, 1.1 g) in 5 mL MeOH for 1 h at room temperature. The reaction mixture was added 10 mL saturated $NaHCO_3$ solution, filtered and washed the solid with water. Then the crude product was recrystallized in MeOH to get the target product **A6** as white solid with 54% yield, mp: 283-286□. ^{1}H NMR (400 MHz, DMSO-d_6, ppm): δ 8.12 (d, J = 5.6 Hz, 1H, C_6-thienopyrimidine-H), 7.78 (d, J = 8.2 Hz, 2H, C_3,C_5-Ph-H), 7.70 (s, 2H, C_3,C_5-Ph'-H), 7.47 (d, J = 8.1 Hz, 2H, C_2,C_6-Ph-H), 7.27 (s, 2H, SO_2NH_2), 7.16 (d, J = 5.3 Hz, 1H, C_7-thienopyrimidine-H), 6.74 (s, 1H,

NH), 4.15 (s, 1H), 3.77-3.74 (m, 1H), 3.48 (s, 2H, N-CH_2), 2.72 (s, 2H), 2.11 (s, 6H), 2.03-1.91 (m, 2H), 1.80-1.40 (m, 4H). ^{13}C NMR (100 MHz, DMSO-d_6): δ 165.4, 162.0, 160.2, 153.4, 143.3, 136.7, 133.5, 132.2, 129.8, 126.4, 123.8, 119.5, 109.2, 82.5, 81.0, 61.9, 52.8, 31.6, 16.2. ESI-MS: m/z 548.2 $[M + 1]^+$. $C_{28}H_{29}N_5O_3S_2$ (547.17).

General procedure for the preparation of AXNX

Compound **A1-A6** (0.5 mmol) and a variety of azide substituents (0.6 mmol) were added in a mixed solution of water and DMF (v/v= 1:1, 10 mL). Then a solution of 1 M freshly prepared sodiumascorbate (0.195 mmol, 0.04 g) and 7.5% $CuSO_4 \cdot 5H_2O$ (0.065 mmol, 0.017 g) in water were added to the mixture. The heterogeneous mixture was stirred vigorously at 50□ for 4-12 h (monitored by TLC). Then 20 mL water was added to the mixture and extracted with ethyl acetate (3 × 10 mL). The organic phase was dried over anhydrous Na_2SO_4, filtered, and purified by flash column chromatography. The product was recrystallized from ethyl acetate/petroleum ether to afford the target compound **AXNX.**

4-((2-((1-((1-(2-cyanobenzyl)-1*H*-1,2,3-triazol-4-yl)methyl)piperidin-4-yl) amino)thieno[3,2-*d*]pyrimidin-4-yl)oxy)-3,5-dimethylbenzonitrile (A3N1)

White solid, 92% yield, mp: 149-151°C. ^{1}H NMR (400 MHz, DMSO-d_6) δ 8.20 (d, J = 5.4 Hz, 1H, C_6-thienopyrimidine-H), 8.08 (s, 1H, triazol-H), 7.92 (dd, J = 7.7, 1.4 Hz, 1H, C_3-Ph-H), 7.73 (d, J = 1.5 Hz, 1H, C_5-Ph-H), 7.72 (s, 2H, C_3,C_5-Ph'-H), 7.60-7.55 (m, 1H, C_6-Ph-H), 7.36 (d, J = 7.8 Hz, 1H, C_4 -Ph-H), 7.26-7.25 (m, 1H, C_7-thienopyrimidine-H), 6.88 (s, 1H, NH), 5.80 (s, 2H, triazol-CH_2), 3.71 (s, 1H),

3.56 (s, 2H, N-CH_2), 2.80 (s, 2H), 2.11 (s, 6H), 1.72-1.53 (m, 3H), 1.45-1.39 (m, 3H). ^{13}C NMR (100 MHz, DMSO-d_6) δ 162.4, 153.4, 139.4, 134.3, 133.8, 133.2, 133.0, 129.8, 129.6, 124.9, 119.0, 117.4, 111.6, 109.0, 52.9, 52.3, 51.4, 39.6, 31.5, 16.2. ESI-MS: m/z 576.6 $[M + 1]^+$. $C_{31}H_{29}N_9OS$ (575.22).

4-((2-((1-((1-(4-cyanobenzyl)-1*H*-1,2,3-triazol-4-yl)methyl)piperidin-4-yl) amino)thieno[3,2-*d*]pyrimidin-4-yl)oxy)-3,5-dimethylbenzonitrile (A3N3)

White solid, 90% yield, mp: 140-142°C. ^{1}H NMR (400 MHz, DMSO-d_6) δ 8.20 (d, J = 5.3 Hz, 1H, C_6-thienopyrimidine-H), 8.13 (s, 1H, triazol-H), 7.86 (d, J = 8.0 Hz, 2H, C_3,C_5-Ph-H), 7.72 (s, 2H, C_3,C_5-Ph'-H), 7.44 (d, J = 7.5 Hz, 2H, C_2,C_6-Ph-H), 7.27 (s, 1H, C_7-thienopyrimidine-H), 6.87 (s, 1H, NH), 5.73 (s, 2H, triazol-CH_2), 3.72-3.71 (s, 1H), 3.54 (s, 2H, N-CH_2), 2.79 (s, 2H), 2.11 (s, 6H), 1.91-1.57 (m, 4H), 1.45-1.39 (s, 2H). ^{13}C NMR (100 MHz, DMSO-d_6) δ 162.4, 153.4, 139.4, 134.3, 133.8, 133.2, 133.0, 129.8, 129.6, 124.9, 119.0, 117.4, 111.6, 109.0, 52.9, 52.3, 51.4, 39.6, 31.5, 16.2. ESI-MS: m/z 576.6 $[M + 1]^+$. $C_{31}H_{29}N_9OS$ (575.22).

3,5-dimethyl-4-((2-((1-((1-(2-nitrobenzyl)-1*H*-1,2,3-triazol-4-yl)methyl) piperidin-4-yl)amino)thieno[3,2-*d*]pyrimidin-4-yl)oxy)benzonitrile (A3N4)

White solid, 93% yield, mp: 155-157°C. ^{1}H NMR (400 MHz, DMSO-d_6) δ 8.21 (d, J = 5.4 Hz, 1H, C_6-thienopyrimidine-H), 8.19-8.17 (m, 1H), 8.01 (s, 1H, triazol-H), 7.72 (s, 2H, C_3,C_5-Ph'-H), 7.62-7.55 (m, 2H), 7.32-7.31 (m, 2H), 7.26-7.24 (m, 1H, C_7-thienopyrimidine-H), 6.88 (s, 1H, NH), 5.80 (s, 2H, triazol-CH_2), 3.70 (s, 1H), 3.52 (s, 2H, N-CH_2), 2.80 (s, 2H), 2.11 (s, 6H), 1.85-1.60 (m, 4H), 1.42-1.31 (m, 2H). ^{13}C NMR (100 MHz, DMSO-d_6) δ 162.4, 153.4, 139.7, 134.3, 133.8, 133.2, 133.0,

129.8, 124.9, 119.0, 117.4, 111.6, 109.0, 52.9, 52.3, 51.3, 39.6, 31.5, 16.2. ESI-MS: m/z 596.4 $[M + 1]^+$. $C_{30}H_{29}N_9O_3S$ (595.21).

3,5-dimethyl-4-((2-((1-((1-(2-methylbenzyl)-1*H*-1,2,3-triazol-4-yl)methyl) piperidin-4-yl)amino)thieno[3,2-*d*]pyrimidin-4-yl)oxy)benzonitrile (A3N10)

White solid, 88% yield, mp: 114-116°C. ^{1}H NMR (400 MHz, DMSO-d_6) δ 8.20 (d, J = 5.4 Hz, 1H, C_6-thienopyrimidine-H), 7.91 (s, 1H, triazol-H), 7.71 (s, 2H, C_3,C_5-Ph'-H), 7.28-7.18 (m, 4H), 7.05 (d, J = 7.4 Hz, 1H), 6.87 (s, 1H, NH), 5.58 (s, 2H, triazol-CH_2), 3.68 (s, 1H), 3.52 (s, 2H, N-CH_2), 2.77 (s, 2H), 2.30 (s, 3H), 2.11 (s, 6H), 1.90-1.39 (m, 6H). ^{13}C NMR (100 MHz, DMSO-d_6) δ 162.4, 153.4, 136.6, 134.8, 133.2, 130.8, 128.9, 128.7, 126.7, 124.9, 119.0, 117.4, 111.6, 109.0, 53.0, 52.3, 51.3, 39.6, 31.5, 19.1, 16.2. ESI-MS: m/z 565.6 $[M + 1]^+$. $C_{31}H_{32}N_8OS$ (564.24).

3,5-dimethyl-4-((2-((1-((1-(4-methylbenzyl)-1*H*-1,2,3-triazol-4-yl)methyl) piperidin-4-yl)amino)thieno[3,2-*d*]pyrimidin-4-yl)oxy)benzonitrile (A3N12)

White solid, 84% yield, mp: 112-114°C. ^{1}H NMR (400 MHz, DMSO-d_6) δ 8.20 (d, J = 5.4 Hz, 1H, C_6-thienopyrimidine-H), 7.98 (s, 1H, triazol-H), 7.71 (s, 2H, C_3,C_5-Ph'-H), 7.25-7.12 (m, 5H), 6.87 (s, 1H, NH), 5.51 (s, 2H, triazol-CH_2), 3.68 (s, 1H), 3.50 (s, 2H, N-CH_2), 2.76 (s, 2H), 2.28 (s, 3H), 2.11 (s, 6H), 1.87-1.62 (m, 3H), 1.50- 1.39 (m, 3H). ^{13}C NMR (100 MHz, DMSO-d_6) δ 162.4, 153.4, 139.4, 137.8, 134.3, 133.6, 133.2, 129.7, 128.3, 124.9, 119.0, 117.8, 109.0, 52.9, 52.3, 31.5, 21.1, 16.2. ESI-MS: m/z 565.6 $[M + 1]^+$. $C_{31}H_{32}N_8OS$ (564.24).

4-((4-((4-((4-(4-cyano-2,6-dimethylphenoxy)thieno[3,2-*d*]pyrimidin-2-yl) amino)piperidin-1-yl)methyl)-1*H*-1,2,3-triazol-1-yl)methyl)benzenesulfonamide

(A3N18)

White solid, 93% yield, mp: 186-188°C. ^{1}H NMR (400 MHz, DMSO-d_6) δ 8.20 (d, J = 5.4 Hz, 1H, C_6-thienopyrimidine-H), 8.07 (s, 1H, triazol-H), 7.82 (d, J = 8.2 Hz, 2H, C_3,C_5-Ph-H), 7.72 (s, 2H, C_3,C_5-Ph'-H), 7.46 (d, J = 8.0 Hz, 2H, C_2,C_6-Ph-H), 7.38 (s, 2H, SO_2NH_2), 7.26 (s, 1H, C_7-thienopyrimidine-H), 6.87 (s, 1H, NH), 5.67 (s, 2H, triazol-CH_2), 3.69 (s, 1H), 3.52 (s, 2H, N-CH_2), 2.76 (s, 2H), 2.11 (s, 6H), 1.89-1.52 (m, 4H), 1.46-1.22 (m, 2H). ^{13}C NMR (100 MHz, DMSO-d_6) δ 162.4, 153.4, 144.5, 144.2, 140.4, 139.4, 133.2, 133.0, 129.8, 128.7, 126.5, 124.5, 119.0, 117.6, 112.1, 109.0, 53.1, 52.5, 52.4, 39.6, 31.6, 16.2. ESI-MS: m/z 630.5 $[M + 1]^+$. $C_{30}H_{31}N_9O_3S_2$ (629.20).

4-((4-((4-((4-(4-cyano-2,6-dimethylphenoxy)thieno[3,2-*d*]pyrimidin-2-yl) amino)piperidin-1-yl)methyl)-1*H*-1,2,3-triazol-1-yl)methyl)benzamide (A3N19)

White solid, 91% yield, mp: 200-202°C. ^{1}H NMR (400 MHz, DMSO-d_6) δ 8.20 (d, J = 5.4 Hz, 1H, C_6-thienopyrimidine-H), 8.05 (s, 1H, triazol-H), 7.86 (d, J = 8.0 Hz, 2H, C_2,C_6-Ph-H), 7.71 (s, 2H, C_3,C_5-Ph'-H), 7.40 (s, 2H, $CONH_2$), 7.34 (d, J = 8.0 Hz, 2H, C_3,C_5-Ph-H), 7.27 (s, 1H, C_7-thienopyrimidine-H), 6.87 (s, 1H, NH), 5.63 (s, 2H, triazol-CH_2), 3.69 (s, 1H), 3.51 (s, 2H, N-CH_2), 2.77 (s, 2H), 2.11 (s, 6H), 1.91-1.72 (m, 3H), 1.51-1.23 (m, 3H). ^{13}C NMR (100 MHz, DMSO-d_6) δ 167.8, 165.4, 162.8, 153.1, 144.5, 139.7, 134.4, 133.2, 133.0, 128.3, 128.0, 126.1, 124.4, 119.0, 117.1, 112.5, 109.8, 53.1, 52.7, 52.4, 39.6, 31.6, 16.2. ESI-MS: m/z 594.6 $[M + 1]^+$. $C_{31}H_{31}N_9O_2S$ (593.23).

2-(4-((4-((4-(4-cyano-2,6-dimethylphenoxy)thieno[3,2-*d*]pyrimidin-2-yl)

amino)piperidin-1-yl)methyl)-1H-1,2,3-triazol-1-yl)-*N*-(4-(methylsulfonyl) phenyl)acetamide (A3N24)

White solid, 93% yield, mp: 173-175°C. ^{1}H NMR (400 MHz, DMSO-d_6) δ 10.93 (s, 1H, CONH), 8.20 (d, J = 5.4 Hz, 1H, C_6-thienopyrimidine-H), 8.00 (s, 1H, triazol-H), 7.90 (d, J = 8.7 Hz, 2H, C_3,C_5-Ph-H), 7.82 (d, J = 8.7 Hz, 2H, C_2,C_6-Ph-H), 7.72 (s, 2H, C_3,C_5-Ph'-H), 7.28 (s, 1H, C_7-thienopyrimidine-H), 6.88 (s, 1H, NH), 5.38 (s, 2H, triazol-CH_2), 3.62-3.48 (m, 3H), 3.18 (s, 3H), 2.85-2.82 (m, 2H), 2.11 (s, 6H), 1.91- 1.55 (m, 4H), 1.43-1.17 (m, 2H). ^{13}C NMR (100 MHz, DMSO-d_6) δ 165.7, 162.4, 153.4, 143.3, 140.3, 139.8, 135.6, 133.2, 128.8, 126.5, 124.5, 119.5, 117.1, 112.5, 109.8, 52.6, 52.3, 44.2, 39.4, 31.6, 16.2. ESI-MS: m/z 672.3 $[M + 1]^+$. $C_{32}H_{33}N_9O_4S_2$ (671.21).

4-((2-((1-((1-((2S,3S,5S)-2-(hydroxymethyl)-5-(5-methyl-2,4-dioxo-3,4-dihydropyrimidin-1(2*H*)-yl)tetrahydrofuran-3-yl)-1*H*-1,2,3-triazol-4-yl) methyl)piperidin-4-yl)amino)thieno[3,2-*d*]pyrimidin-4-yl)oxy)-3,5-dimethylbenzonitrile (A3N33)

White solid, 87% yield, mp: 251-253°C. ^{1}H NMR (400 MHz, DMSO-d_6) δ 11.23 (s, 1H, NH), 8.20 (d, J = 5.4 Hz, 1H, C_6-thienopyrimidine-H), 8.05 (s, 1H, triazol-H), 7.71 (s, 2H, C_3,C_5-Ph-H), 7.21 (s, 1H), 7.27 (s, 1H, C_7-thienopyrimidine-H), 6.87 (s, 1H, NH), 5.86 (s, 1H), 5.63 (s, 2H, triazol-CH_2), 4.96 (s, 1H, OH), 3.97 (s, 1H), 3.69 (s, 1H), 3.51-3.49 (m, 2H), 2.76 (s, 2H), 2.63-2.48 (m, 2H), 2.36 (s, 3H), 2.11 (s, 6H), 1.87-1.71 (m, 3H), 1.60-1.27 (m, 3H). ^{13}C NMR (100 MHz, DMSO-d_6) δ 167.8, 165.4, 162.8, 153.1, 144.5, 139.7, 134.4, 133.2, 128.3, 126.1, 124.4, 119.0, 112.5,

109.8, 94.5, 77.8, 70.5, 53.1, 52.7, 52.4, 39.6, 37.1, 31.6, 16.2, 12.4. ESI-MS: m/z 685.6 $[M + 1]^+$. $C_{33}H_{36}N_{10}O_5S$ (684.78).

3,5-dimethyl-4-((2-((1-((1-(2-morpholino-2-oxoethyl)-1H-1,2,3-triazol-4-yl)methyl)piperidin-4-yl)amino)thieno[3,2-*d*]pyrimidin-4-yl)oxy)benzonitrile (A3N34)

White solid, 93% yield, mp: 228-230°C. ^{1}H NMR (400 MHz, DMSO-d_6) δ 8.20 (d, *J* = 5.4 Hz, 1H, C_6-thienopyrimidine-H), 7.84 (s, 1H, triazol-H), 7.72 (s, 2H, C_3,C_5-Ph-H), 7.27 (s, 1H, C_7-thienopyrimidine-H), 6.87 (s, 1H, NH), 5.44 (s, 2H, triazol-CH_2), 3.64 (d, *J* = 4.8 Hz, 2H), 3.59 (t, *J* = 4.9 Hz, 3H), 3.53 (d, *J* = 5.2 Hz, 4H), 3.46 (d, *J* = 4.8 Hz, 2H), 2.79 (s, 2H), 2.11 (s, 6H), 1.90-1.51 (m, 4H), 1.47-1.23 (m, 2H). ^{13}C NMR (100 MHz, DMSO-d_6) δ 165.0, 162.3, 153.7, 143.3, 140.3, 139.8, 135.6, 133.2, 125.8, 117.5, 112.1, 109.6, 66.4, 66.3, 53.1, 52.3, 50.9, 45.1, 42.3, 31.6, 16.2. ESI-MS: m/z 588.5 $[M + 1]^+$. $C_{29}H_{33}N_9O_3S$ (587.24).

3,5-dimethyl-4-((2-((1-((1-(2-oxo-2-(pyrrolidin-1-yl)ethyl)-1H-1,2,3-triazol-4-yl)methyl)piperidin-4-yl)amino)thieno[3,2-*d*]pyrimidin-4-yl)methyl)benzonitrile (A3N35)

White solid, 91% yield, mp: 219-221°C. ^{1}H NMR (400 MHz, DMSO-d_6) δ 8.20 (d, *J* = 5.4 Hz, 1H, C_6-thienopyrimidine-H), 7.84 (s, 1H, triazol-H), 7.72 (s, 2H, C_3,C_5-Ph'-H), 7.27 (s, 1H, C_7-thienopyrimidine-H), 6.87 (s, 1H, NH), 5.31 (s, 2H, triazol-CH_2), 3.69 (s, 1H), 3.52 (t, *J* = 6.8 Hz, 4H), 3.51-3.47 (s, 2H, N-CH_2), 3.40-3.24 (m, 4H), 2.79 (s, 2H), 2.11 (s, 6H), 2.02-1.62 (m, 4H), 1.53-1.39 (s, 2H). ^{13}C NMR (100 MHz, DMSO-d_6) δ 164.2, 162.1, 153.0, 143.6, 140.1, 139.5, 135.6,

133.2, 133.0, 125.7, 119.0, 53.0, 52.3, 51.6, 46.2, 45.5, 39.6, 31.6, 26.0, 24.1, 16.2. ESI-MS: m/z 572.5 $[M + 1]^+$. $C_{29}H_{33}N_9O_2S$ (571.25).

4-((4-((4-(4-(1-(4-chlorobenzyl)-1*H*-1,2,3-triazol-4-yl)-2,6-dimethylphenoxy) thieno[3,2-*d*]pyrimidin-2-yl)amino)piperidin-1-yl)methyl)benzenesulfonamide (A6N9)

White solid, 87% yield, mp: 241-242°C. ^{1}H NMR (400 MHz, DMSO-d_6, ppm): δ 8.17 (d, J = 5.4 Hz, 1H, C_6-thienopyrimidine-H), 7.84 (s, 1H, triazol-H), 7.76 (d, J = 8.3 Hz, 2H, C_3,C_5-Ph-H), 7.71 (s, 2H, C_3,C_5-Ph'-H), 7.50 (d, J = 7.8 Hz, 2H, C_3,C_5-Ph''-H), 7.43 (d, J = 8.2 Hz, 2H, C_2,C_6-Ph-H), 7.29 (s, 2H, SO_2NH_2), 7.25 (d, J = 5.3 Hz, 1H, C_7-thienopyrimidine-H), 7.24 (d, J = 8.4 Hz, 2H, C_2,C_6-Ph''-H), 6.87 (s, 1H, NH), 5.31 (s, 2H, triazol-CH_2), 3.73-3.72 (m, 1H), 3.48 (s, 2H, N-CH_2), 2.72-2.70 (m, 2H), 2.12 (s, 6H), 1.90-1.42 (m, 6H). ^{13}C NMR (100 MHz, DMSO-d_6): δ 165.3, 162.5, 160.7, 153.4, 143.8, 143.1, 140.8, 136.7, 135.7, 133.2, 133.0, 129.4, 128.7, 126.0, 123.9, 123.2, 119.0, 109.3, 62.1, 53.2, 52.8, 31.8, 16.2. ESI-MS: m/z 715.1 $[M + 1]^+$. $C_{35}H_{35}ClN_8O_3S_2$ (714.20).

4-((4-((4-(2,6-dimethyl-4-(1-(2-(thiophen-3-yl)ethyl)-1H-1,2,3-triazol-4-yl) phenoxy)thieno[3,2-*d*]pyrimidin-2-yl)amino)piperidin-1-yl)methyl) benzenesulfonamide (A6N17)

White solid, 91% yield, mp: 216-217°C. ^{1}H NMR (400 MHz, DMSO-d_6, ppm): δ 8.18 (d, J = 5.3 Hz, 1H, C_6-thienopyrimidine-H), 7.83 (s, 1H, triazol-H), 7.76 (d, J = 8.3 Hz, 2H, C_3,C_5-Ph-H), 7.72 (s, 2H, C_3,C_5-Ph'-H), 7.45 (d, J = 8.2 Hz, 2H, C_2,C_6-Ph-H), 7.28 (s, 2H, SO_2NH_2), 7.25-7.23 (m, 2H), 6.92-6.89 (m, 2H), 6.87 (s,

1H, NH), 3.97-3.95 (m, 2H), 3.74 (s, 1H), 3.48 (s, 2H, N-CH_2), 3.10-3.08 (m, 2H), 2.72 (s, 2H), 2.11 (s, 6H), 1.91-1.39 (m, 6H). ESI-MS: m/z 701.3 $[M + 1]^+$. $C_{34}H_{36}N_8O_3S_3$ (700.21).

4-((4-((4-(2,6-dimethyl-4-(1-(2-oxo-2-(pyrrolidin-1-yl)ethyl)-1H-1,2,3-triazol-4-yl)phenoxy)thieno[3,2-*d*]pyrimidin-2-yl)amino)piperidin-1-yl)methyl) Benzenesulfonamide (A6N35)

White solid, 95% yield, mp: 233-235°C. ^{1}H NMR (400 MHz, DMSO-d_6, ppm): δ 8.17 (d, J = 5.3 Hz, 1H, C_6-thienopyrimidine-H), 7.83 (s, 1H, triazol-H), 7.76 (d, J = 8.4 Hz, 2H, C_3,C_5-Ph-H), 7.72 (s, 2H, C_3,C_5-Ph'-H), 7.45 (d, J = 8.3 Hz, 2H, C_2,C_6-Ph-H), 7.28 (s, 2H, SO_2NH_2), 7.23 (d, J = 5.4 Hz, 1H, C_7-thienopyrimidine-H), 6.84 (s, 1H, NH), 5.62-5.60 (m, 2H, $COCH_2$), 3.74 (s, 1H), 3.48 (s, 2H, N-CH_2), 3.10-3.09 (m, 4H), 2.74-2.72 (s, 2H), 2.10 (s, 6H), 1.98-1.41 (m, 10H). ^{13}C NMR (100 MHz, DMSO-d_6): δ 172.4, 165.2, 162.9, 160.5, 153.4, 143.7, 136.7, 133.2, 132.9, 129.2, 126.6, 123.8, 121.5, 119.0, 109.2, 61.9, 57.2, 52.8, 48.4, 31.7, 25.7, 16.2. ESI-MS: m/z 702.2 $[M + 1]^+$. $C_{34}H_{39}N_9O_4S_2$ (701.26).

4.2 Biological evaluation

4.2.1 Recombinant HIV-1 RT inhibitory assays

The HIV-RT inhibition assay was performed by using the ELISA method.[27] Briefly, the reaction mixture containing HIV-1 RT enzyme, reconstituted template and viral nucleotides [digoxigenin (DIG)-dUTP, biotin-dUTP and dTTP] in the buffer with or without inhibitors was incubated at 37ºC for 1 h. Then, the mixture was transferred to a streptavidin-coated microtitre plate (MTP) and incubated for another 2 h at 37ºC.

The biotin-labeled dNTPs bound to streptavidin under RT conditions to form a cDNA chain. The unbound dNTPs were washed with washing buffer, and then anti-DIG-POD was added to the MTPs. After incubation for another 1 h at 37ºC, the DIG-labeled dNTPs incorporated in cDNA were bound to the anti-DIG-POD antibody. The unbound anti-DIG-PODs were washed out and the peroxide substrate (ABST) solution was added. The absorbance was determined at OD405 nm wiht a microtiter plate ELISA reader. The percentage inhibitory activity of RT inhibitors was calculated according to the following formula:

% Inhibition = [O.D. value with RT but without inhibitors - O.D. value with RT and inhibitors]/[O.D. value with RT and inhibitors - O.D. value without RT and inhibitors].

4.2.2 *In vitro* anti-HIV-1 assay

The anti-HIV-1 activity assay were performed in MT-4 cells using the MTT method.[28] The compounds stock solutions (10 × final concentration) were added in 25 µL volumes to two series of triplicate wells with the aim to allow simultaneous evaluation of their effects on mock- and HIV-infected cells at the beginning of each experiment. Serial 5-fold dilutions of compounds were made directly in flat-bottomed 96-well microtiter trays using a Biomek 3000 robot (Beckman instruments, Fullerton, CA). Untreated HIV- and mock-infected cell samples were included as controls. HIV stock (50 µL) at 100-300 $CCID_{50}$ (50 % cell culture infectious doses) or culture medium was added to either the infected or mock-infected cell wells of the microtiter tray. Mock-infected cells were used to evaluate the effects of test compound on

uninfected cells to assess the cytotoxicity of the compounds. Exponentially growing MT-4 cells were centrifuged for 5 minutes at 220 g and the supernatant was discarded. The MT-4 cells were resuspended at 6×10^5 cells/mL and 50 µL volumes were transferred to the microtiter tray wells. Five days after infection, the viability of mock-and HIV-infected cells was examined spectrophotometrically using the MTT assay. The absorbances were read in an eight-channel computer-controlled photometer (Infinite M1000, Tecan), at two wavelengths (540 and 690 nm). All data were calculated using the median absorbance value of three wells. The 50% cytotoxic concentration (CC_{50}) was defined as the concentration of the compounds that reduced the absorbance (OD_{540}) of the mock-infected control sample by 50%. The concentration achieving 50% protection against the cytopathic effect of the virus in infected cells was defined as the 50% effective concentration (EC_{50}).

4.3 Molecular simulation studies

The Sybyl-X 2.0 software was used to perform the molecular modelling studies. [26]All the molecules for docking were built using standard bond lengths and angles from Sybyl-X 2.0/Base Builder and were optimized using the Tripos force field for 1000 generations two times or more, until the minimized conformers of the ligand were the same. The flexible docking method (Surflex-Dock) docks the ligand automatically into the ligand-binding site of the receptor by using a protocol-based approach and an empirically derived scoring function. The protocol is a computational representation of a putative ligand that binds to the intended binding site and is a unique and essential element of the docking algorithm. The scoring function in

Surflex-Dock, containing hydrophobic, polar, repulsive, entropic, and solvation terms, was trained to estimate the dissociation constant (Kd). The protein was prepared by removing the ligand and other unnecessary small molecules from the cocrystal structure (PDB code: 6c0n), polar hydrogen atoms and charges were added to the protein before docking. During the docking procedure, all of the single bonds in residue side-chains inside the defined RT binding pocket were regarded as rotatable or flexible, and the ligand was allowed to rotate at all single bonds and to move flexibly within the tentative binding pocket. The atomic charges were recalculated using the Kollman all-atom approach for the protein and the Gasteiger-Hückel approach for the ligand. The binding interaction energy was calculated, including van der Waals, electrostatic, and torsional energy terms defined in the Tripos force field. The structure optimization was performed for 10,000 generations using a genetic algorithm, and the 20-best-scoring ligand-protein complexes were kept for further analysis. The -log $(Kd)^2$ values of the 20-best-scoring complexes, representing the binding affinities of ligand with RT, encompassed a wide range of functional classes (10^{-2}-10^{-9}). The highest-scoring 3D structural model of ligand-bound RT was chosen to define the binding interaction.

Author contributions

All authors contributed to writing the manuscript. All authors have given approval to the final version of the manuscript.

Notes

The authors declare no competing financial interest.

ACKNOWLEDGMENTS

We acknowledge financial support from the National Natural Science Foundation of China (NSFC Nos. 81573347, 81973181, 81903453), China Postdoctoral Science Foundation (2019T120596), Shandong Provincial Natural Science Foundation (ZR2019BH011), Natural Science Foundation of Jiangsu Province (BK2019041035), Young Scholars Program of Shandong University (YSPSDU No. 2016WLJH32), Shandong Provincial Key research and development project (Nos. 2017CXGC1401, 2019JZZY021011), the Taishan Scholar Program at Shandong Province. The technical assistance of Mr. Kris Uyttersprot and Mrs. Kristien Erven, for the HIV experiments is gratefully acknowledged.

REFERENCES

[1] https://www.who.int/hiv/data/en/.

[2] P. Zhan, C. Pannecouque, E. De Clercq, X. Liu, Anti-HIV Drug Discovery and Development: Current Innovations and Future Trends, J. Med. Chem. 59 (2016) 2849-2878.

[3] D. Kang, T. Zhao, Z. Wang, D. Feng, H. Zhang, B. Huang, G. Wu, F. Wei, Z. Zhou, L. Jing, X. Zuo, Y. Tian, V. Poongavanam, J. Kongsted, E. De Clercq, C. Pannecouque, P. Zhan, X. Liu, Discovery of piperidine-substituted thiazolo[5,4-d]pyrimidine derivatives as potent and orally bioavailable HIV-1 non-nucleoside reverse transcriptase inhibitors, Commun. Chem. 2 (2019) 74.

[4] D. Kang, H. Zhang, Z. Wang, T. Zhao, T. Ginex, F.J. Luque, Y. Yang, G. Wu, D. Feng, F. Wei, J. Zhang, E. De Clercq, C. Pannecouque, C.H. Chen, K.H. Lee, N.A. Murugan, T.A. Steitz, P. Zhan, X. Liu, Identification of Dihydrofuro[3,4-d]pyrimidine Derivatives as Novel HIV-1 Non-nucleoside Reverse Transcriptase Inhibitors with Promising Antiviral Activities and Desirable Physicochemical Properties, J. Med. Chem. 62 (2019) 1484-1501.

[5] G. Bec, B. Meyer, M.A. Gerard, J. Steger, K. Fauster, P. Wolff, D. Burnouf, R. Micura, P. Dumas, E. Ennifar, Thermodynamics of HIV-1 reverse transcriptase in action elucidates the mechanism of action of non-nucleoside inhibitors, J. Am. Chem. Soc. 135 (2013) 9743-9752.

[6] V. Namasivayam, M. Vanangamudi, V.G. Kramer, S. Kurup, P. Zhan, X. Liu, J. Kongsted, S.N. Byrareddy, The Journey of HIV-1 Non-Nucleoside Reverse Transcriptase Inhibitors (NNRTIs) from Lab to Clinic, J. Med. Chem. 62 (2019) 4851-4883.

[7] D. Kang, F.X. Ruiz, D. Feng, A. Pilch, T. Zhao, F. Wei, Z. Wang, Y. Sun, Z. Fang, E. De Clercq, C. Pannecouque, E. Arnold, X. Liu, P. Zhan, Discovery and Characterization of Fluorine-Substituted

Diarylpyrimidine Derivatives as Novel HIV-1 NNRTIs with Highly Improved Resistance Profiles and Low Activity for the hERG Ion Channel, J. Med. Chem. 63 (2020) 1298-1312.

[8] C. Beyrer, A. Pozniak, HIV Drug Resistance - An Emerging Threat to Epidemic Control, N. Engl. J. Med. 377 (2017) 1605-1607.

[9] Y. Wang, E. De Clercq, G. Li, Current and emerging non-nucleoside reverse transcriptase inhibitors (NNRTIs) for HIV-1 treatment, Expert Opin. Drug Metab. Toxicol. 15 (2019) 813-829.

[10] W.L. Jorgensen, Efficient Drug Lead Discovery and Optimization, Acc. Chem. Res. 42 (2009) 724-733.

[11] G. Meng, T. Guo, T. Ma, J. Zhang, Y. Shen, K.B. Sharpless, J. Dong, Modular click chemistry libraries for functional screens using a diazotizing reagent, Nature. 574 (2019) 86-89.

[12] X. Wang, B. Huang, X. Liu, P. Zhan, Discovery of bioactive molecules from CuAAC click-chemistry-based combinatorial libraries, Drug Discov. Today. 21 (2016) 118-132.

[13] T. Suzuki, Y. Ota, M. Ri, M. Bando, A. Gotoh, Y. Itoh, H. Tsumoto, P.R. Tatum, T. Mizukami, H. Nakagawa, S. Iida, R. Ueda, K. Shirahige, N. Miyata, Rapid discovery of highly potent and selective inhibitors of histone deacetylase 8 using click chemistry to generate candidate libraries, J. Med. Chem. 55 (2012) 9562-9575.

[14] A.T. Carmona, S. Carrion-Jimenez, V. Pingitore, E. Moreno-Clavijo, I. Robina, A.J. Moreno-Vargas, Harnessing pyrrolidine iminosugars into dimeric structures for the rapid discovery of divalent glycosidase inhibitors, Eur. J. Med. Chem. 151 (2018) 765-776.

[15] X. Jiang, X. Hao, L. Jing, G. Wu, D. Kang, X. Liu, P. Zhan, Recent applications of click chemistry in drug discovery, Expert Opin. Drug Discov. 14 (2019) 779-789.

[16] D. Kang, H. Zhang, Z. Zhou, B. Huang, L. Naesens, P. Zhan, X. Liu, First discovery of novel 3-hydroxy-quinazoline-2,4(1H,3H)-diones as specific anti-vaccinia and adenovirus agents via 'privileged scaffold' refining approach, Bioorg. Med. Chem. Lett. 26 (2016) 5182-5186.

[17] L. Jing, G. Wu, X. Hao, F.A. Olotu, D. Kang, C.H. Chen, K.H. Lee, M.E.S. Soliman, X. Liu, Y. Song, P. Zhan, Identification of highly potent and selective Cdc25 protein phosphatases inhibitors from miniaturization click-chemistry-based combinatorial libraries, Eur. J. Med. Chem. 183 (2019) 111696.

[18] G. Wu, W.A. Zalloum, M.E. Meuser, L. Jing, D. Kang, C.H. Chen, Y. Tian, F. Zhang, S. Cocklin, K.H. Lee, X. Liu, P. Zhan, Discovery of phenylalanine derivatives as potent HIV-1 capsid inhibitors from click chemistry-based compound library, Eur. J. Med. Chem. 158 (2018) 478-492.

[19] P. Gao, L. Sun, J. Zhou, X. Li, P. Zhan, X. Liu, Discovery of novel anti-HIV agents via Cu(I)-catalyzed azide-alkyne cycloaddition (CuAAC) click chemistry-based approach, Expert Opin. Drug Discov. 11 (2016) 857-871.

[20] D. Kang, Z. Fang, Z. Li, B. Huang, H. Zhang, X. Lu, H. Xu, Z. Zhou, X. Ding, D. Daelemans, E. De Clercq, C. Pannecouque, P. Zhan, X. Liu, Design, Synthesis, and Evaluation of Thiophene[3,2-d]pyrimidine Derivatives as HIV-1 Non-nucleoside Reverse Transcriptase Inhibitors with Significantly Improved Drug Resistance Profiles, J. Med. Chem. 59 (2016) 7991-8007.

[21] Y. Yang, D. Kang, L. Nguyen, Z. Smithline, C. Pannecouque, P. Zhan, X. Liu, T.A. Steitz, Structural basis for potent and broad inhibition of HIV-1 RT by thiophene[3,2-d]pyrimidine non-nucleoside inhibitors, eLife. 7 (2018) pii: e36340.

[22] D. Kang, D. Feng, T. Ginex, J. Zou, F. Wei, T. Zhao, B. Huang, Y. Sun, S. Desta, E. De Clercq, C. Pannecouque, P. Zhan, X. Liu, Exploring the hydrophobic channel of NNIBP leads to the discovery of novel piperidine-substituted thiophene[3,2-d]pyrimidine derivatives as potent HIV-1 NNRTIs, Acta Pharm. Sin. B, (2019) https://doi.org/10.1016/j.apsb.2019.1008.1013.

[23] Z. Zhou, T. Liu, G. Wu, D. Kang, Z. Fu, Z. Wang, E. De Clercq, C. Pannecouque, P. Zhan, X. Liu, Targeting the hydrophobic channel of NNIBP: discovery of novel 1,2,3-triazole-derived diarylpyrimidines as novel HIV-1 NNRTIs with high potency against wild-type and K103N mutant virus, Org. Biomol. Chem. 17 (2019) 3202-3217.

[24] B. Huang, W. Chen, T. Zhao, Z. Li, X. Jiang, T. Ginex, D. Vilchez, F.J. Luque, D. Kang, P. Gao, j. Zhang, Y. Tian, D. Daelemans, C.E. De, C. Pannecouque, P. Zhan, X. Liu, Exploiting the Tolerant Region I of the Non-Nucleoside Reverse Transcriptase Inhibitor (NNRTI) Binding Pocket: Discovery of Potent Diarylpyrimidine-Typed HIV-1 NNRTIs against Wild-Type and E138K Mutant Virus with Significantly Improved Water Solubility and Favorable Safety Profiles, J. Med. Chem. 62 (2019) 2083-2098.

[25] Y. Tian, Z. Liu, J. Liu, B. Huang, D. Kang, H. Zhang, E. De Clercq, D. Daelemans, C. Pannecouque, K.H. Lee, C.H. Chen, P. Zhan, X. Liu, Targeting the entrance channel of NNIBP: Discovery of diarylnicotinamide 1,4-disubstituted 1,2,3-triazoles as novel HIV-1 NNRTIs with high potency against wild-type and E138K mutant virus, Eur. J. Med. Chem. 151 (2018) 339-350.

[26] D. Kang, Z. Fang, B. Huang, X. Lu, H. Zhang, H. Xu, Z. Huo, Z. Zhou, Z. Yu, Q. Meng, G. Wu, X. Ding, Y. Tian, D. Daelemans, E. De Clercq, C. Pannecouque, P. Zhan, X. Liu, Structure-Based Optimization of Thiophene[3,2-d]pyrimidine Derivatives as Potent HIV-1 Non-nucleoside Reverse Transcriptase Inhibitors with Improved Potency against Resistance-Associated Variants, J. Med. Chem. 60 (2017) 4424-4443.

[27] A.N. Katchman, J. Koerner, T. Tosaka, R.L. Woosley, S.N. Ebert, Comparative evaluation of HERG currents and QT intervals following challenge with suspected torsadogenic and nontorsadogenic drugs, J. Pharmacol. Exp. Ther. 316 (2006) 1098-1106.

[28] C. Pannecouque, D. Daelemans, E. De Clercq, Tetrazolium-based colorimetric assay for the detection of HIV replication inhibitors: revisited 20 years later, Nat. Protoc. 3 (2008) 427-434.

Graphical abstract

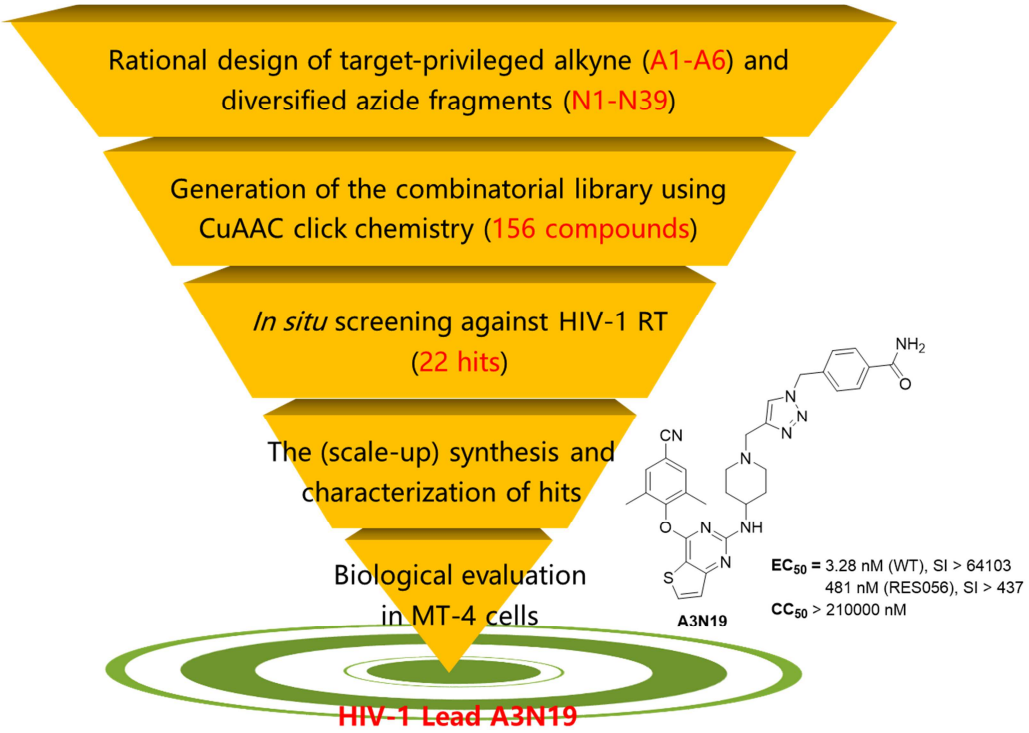

Discovery of potent HIV-1 NNRTIs from CuAAC click-chemistry-based combinatorial libraries

Highlights

1. The technology of rapid assembly and *in situ* screening of focused combinatorial fragment libraries using CuAAC click chemistry was used to discover highly potent HIV-1 NNRTIs for the first time.

2. 22 compounds were identified as anti-HIV-1 hits with improved enzyme inhibitory activity in the *in situ* screening against HIV-1 RT.

3. **A3N19** (EC_{50} = 3.28 nM, SI > 64103) exhibited potent activity than ETR (EC_{50} = 5.1 nM, SI > 889) against HIV-1 IIIB.

Highlights

1. The technology of rapid assembly and *in situ* screening of focused combinatorial fragment libraries using CuAAC click chemistry was used to discover highly potent HIV-1 NNRTIs for the first time.

2. 22 compounds were identified as anti-HIV-1 hits with improved enzyme inhibitory activity in the *in situ* screening against HIV-1 RT.

3. **A3N19** (EC_{50} = 3.28 nM, SI > 64103) exhibited potent activity than ETR (EC_{50} = 5.1 nM, SI > 889) against HIV-1 IIIB.

Declaration of interests

☒ The authors declare that they have no known competing financial interests or personal relationships that could have appeared to influence the work reported in this paper.

☐The authors declare the following financial interests/personal relationships which may be considered as potential competing interests: